US 20160077074A1

(19) **United States**

(12) **Patent Application Publication**

Strong et al.

(10) **Pub. No.: US 2016/0077074 A1**

(43) **Pub. Date: Mar. 17, 2016**

(54) **INTERCONNECTED CORRUGATED CARBON-BASED NETWORK**

(71) Applicant: **The Regents of the University of California**, (US)

(72) Inventors: **Veronica Strong**, Portland, OR (US); **Maher El-Kady**, Culver City, CA (US); **Richard B. Kaner**, Pacific Palisades, CA (US)

(73) Assignee: **THE REGENTS OF THE UNIVERSITY OF CALIFORNIA**, Oakland, CA (US)

(21) Appl. No.: **13/725,073**

(22) Filed: **Dec. 21, 2012**

Related U.S. Application Data

(60) Provisional application No. 61/578,431, filed on Dec. 21, 2011.

Publication Classification

(51) **Int. Cl.**

G01N 33/00	(2006.01)
C01B 31/04	(2006.01)
B32B 18/00	(2006.01)
G21K 5/02	(2006.01)
B32B 3/26	(2006.01)
B32B 3/28	(2006.01)

(52) **U.S. Cl.**

CPC ***G01N 33/0037*** (2013.01); ***B32B 3/26*** (2013.01); ***B32B 3/28*** (2013.01); ***B32B 18/00*** (2013.01); ***G21K 5/02*** (2013.01); ***C01B 31/043*** (2013.01); *B32B 2307/202* (2013.01); *B32B 2457/00* (2013.01); *B32B 2429/02* (2013.01); *C04B 2237/363* (2013.01); *C04B 2237/086* (2013.01); *C04B 2237/592* (2013.01); *C04B 2237/72* (2013.01)

(57) **ABSTRACT**

An interconnected corrugated carbon-based network comprising a plurality of expanded and interconnected carbon layers is disclosed. In one embodiment, each of the expanded and interconnected carbon layers is made up of at least one corrugated carbon sheet that is one atom thick. In another embodiment, each of the expanded and interconnected carbon layers is made up of a plurality of corrugated carbon sheets that are each one atom thick. The interconnected corrugated carbon-based network is characterized by a high surface area with highly tunable electrical conductivity and electrochemical properties.

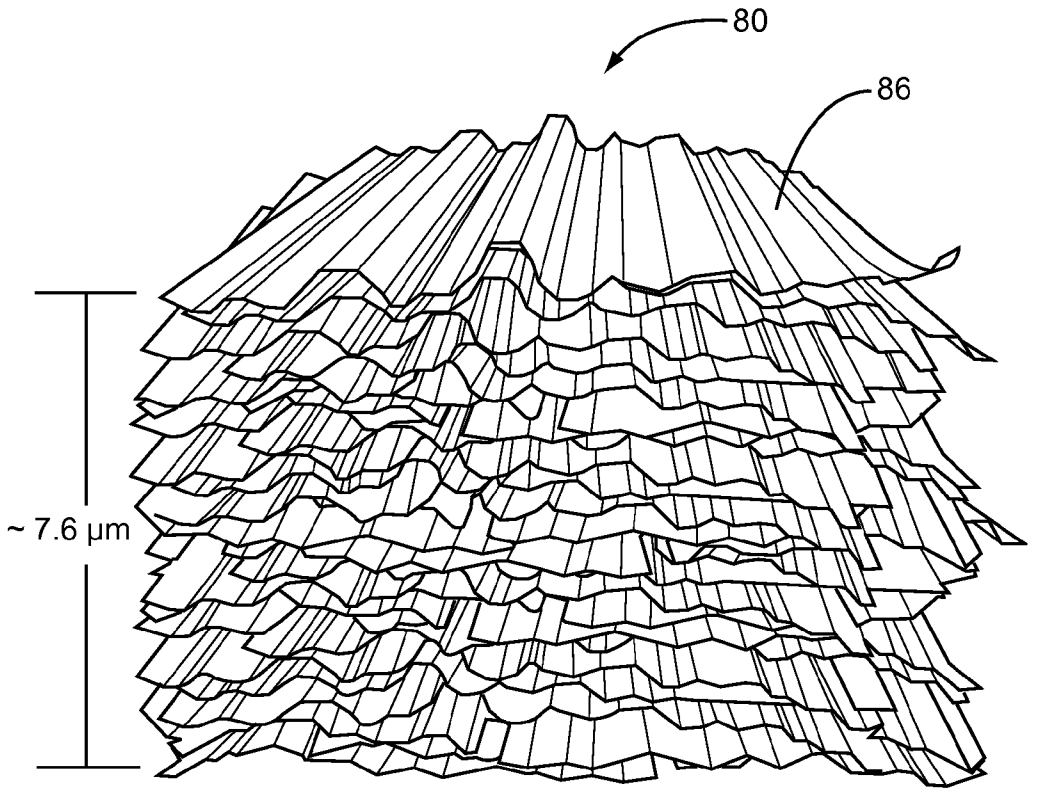

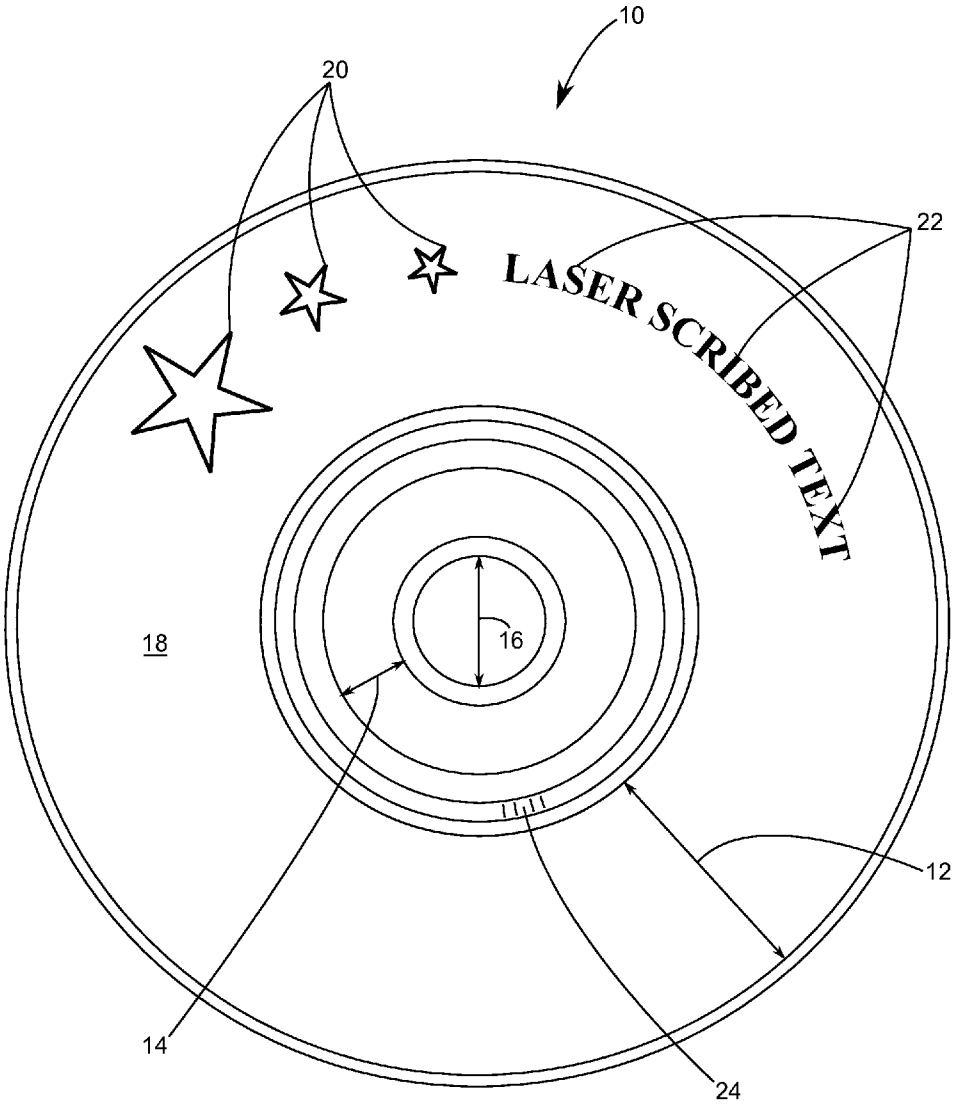

FIG. 1
(PRIOR ART)

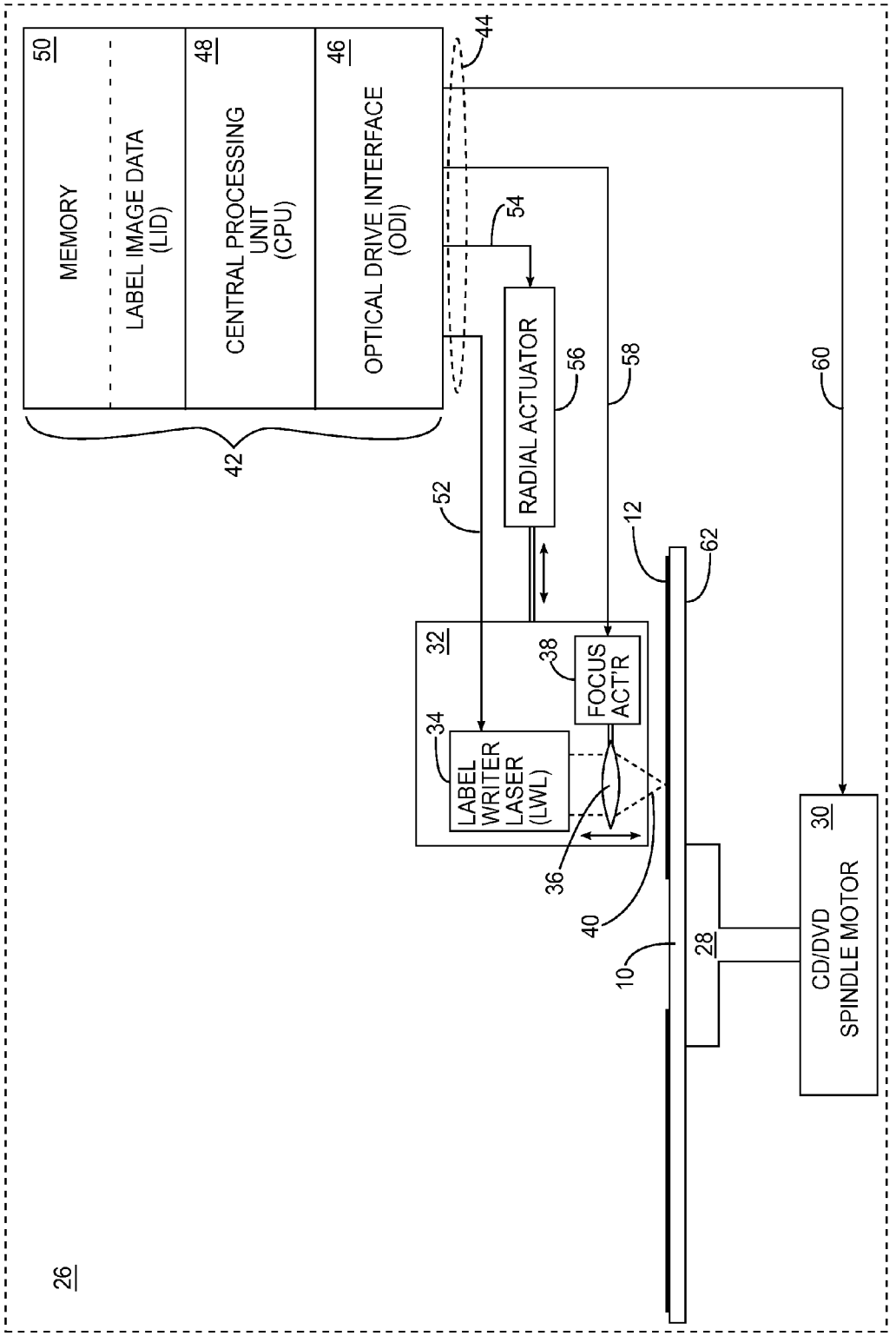

FIG. 2
(PRIOR ART)

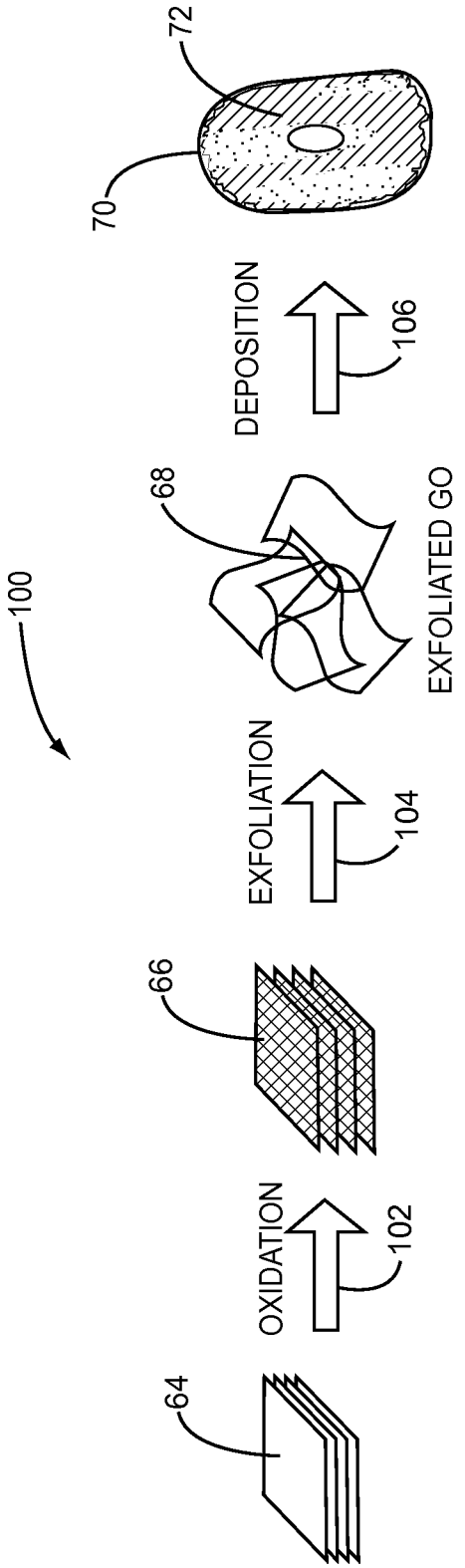
100
64
OXIDATION
102
66
EXFOLIATION
104
68
EXFOLIATED GO
DEPOSITION
106
70
72

FIG. 3

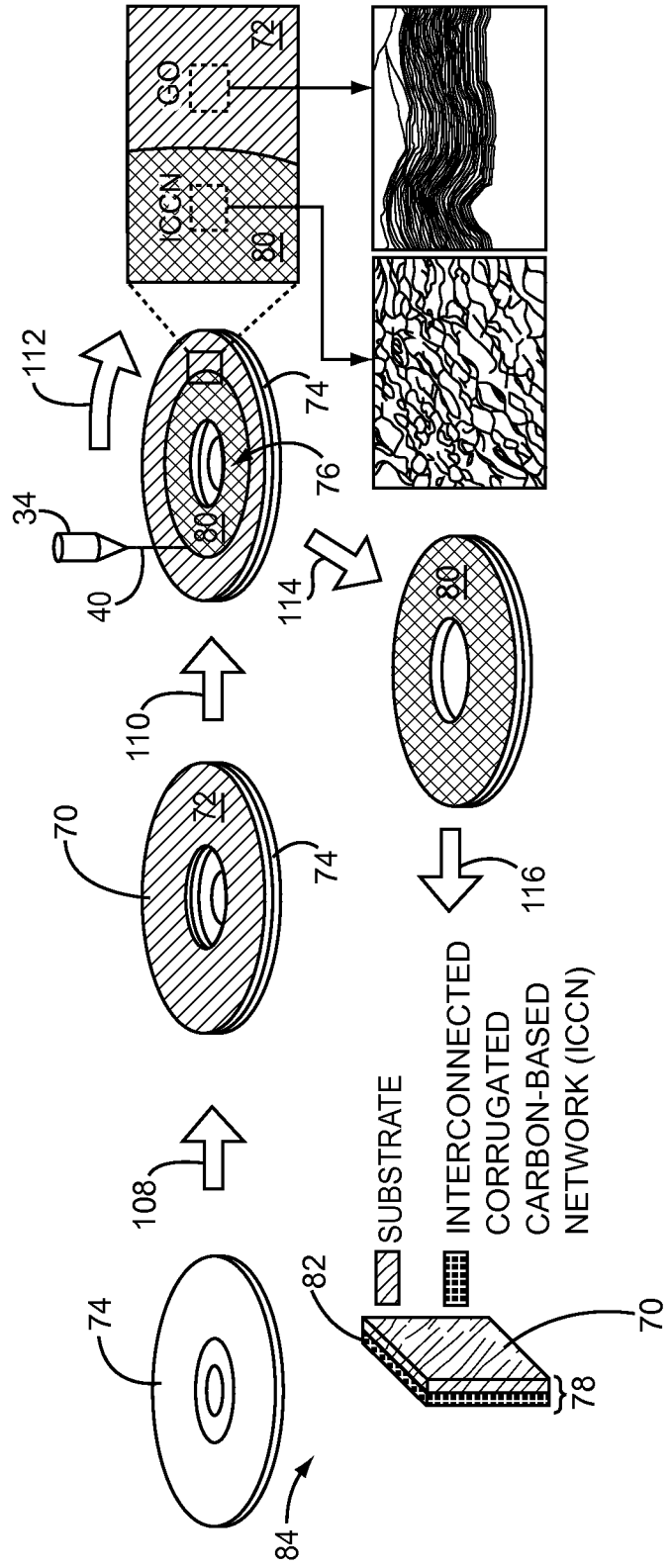
GO
72
ICCN
80
112
74
76
34
40
80
114
110
70
72
74
80
116
108
74
82
SUBSTRATE
INTERCONNECTED CORRUGATED CARBON-BASED NETWORK (ICCN)
70
78
84

FIG. 4

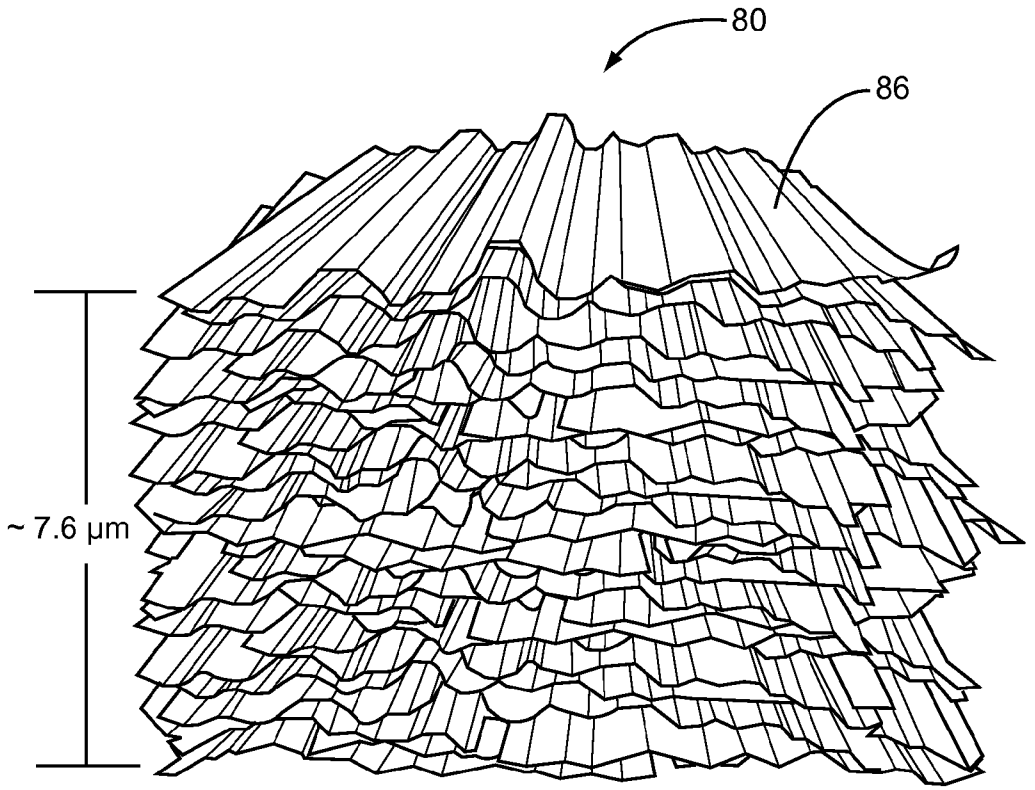

FIG. 5

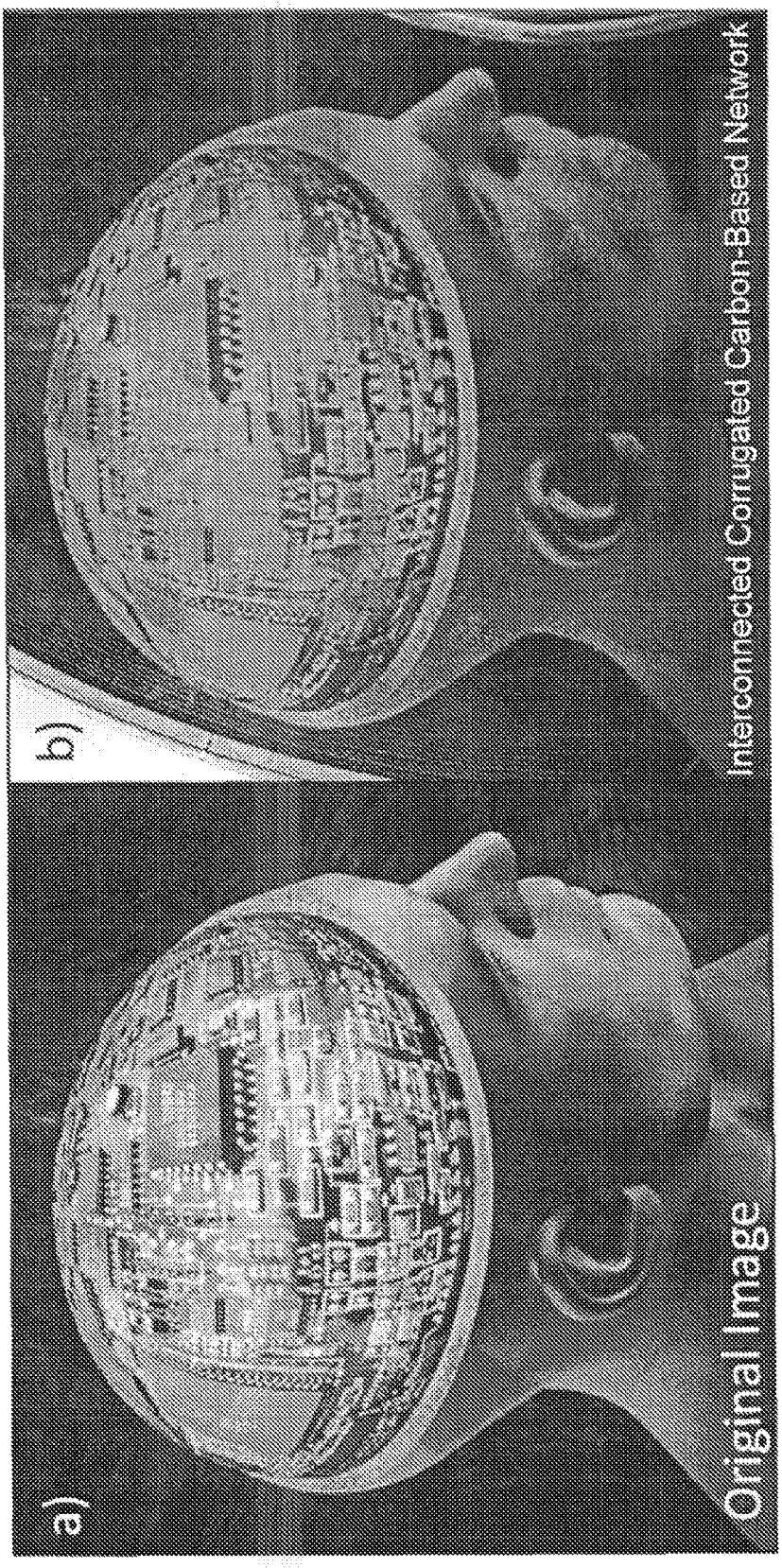
a)
Original Image
b)
Interconnected Corrugated Carbon-Based Network

FIG. 6A

FIG. 6B

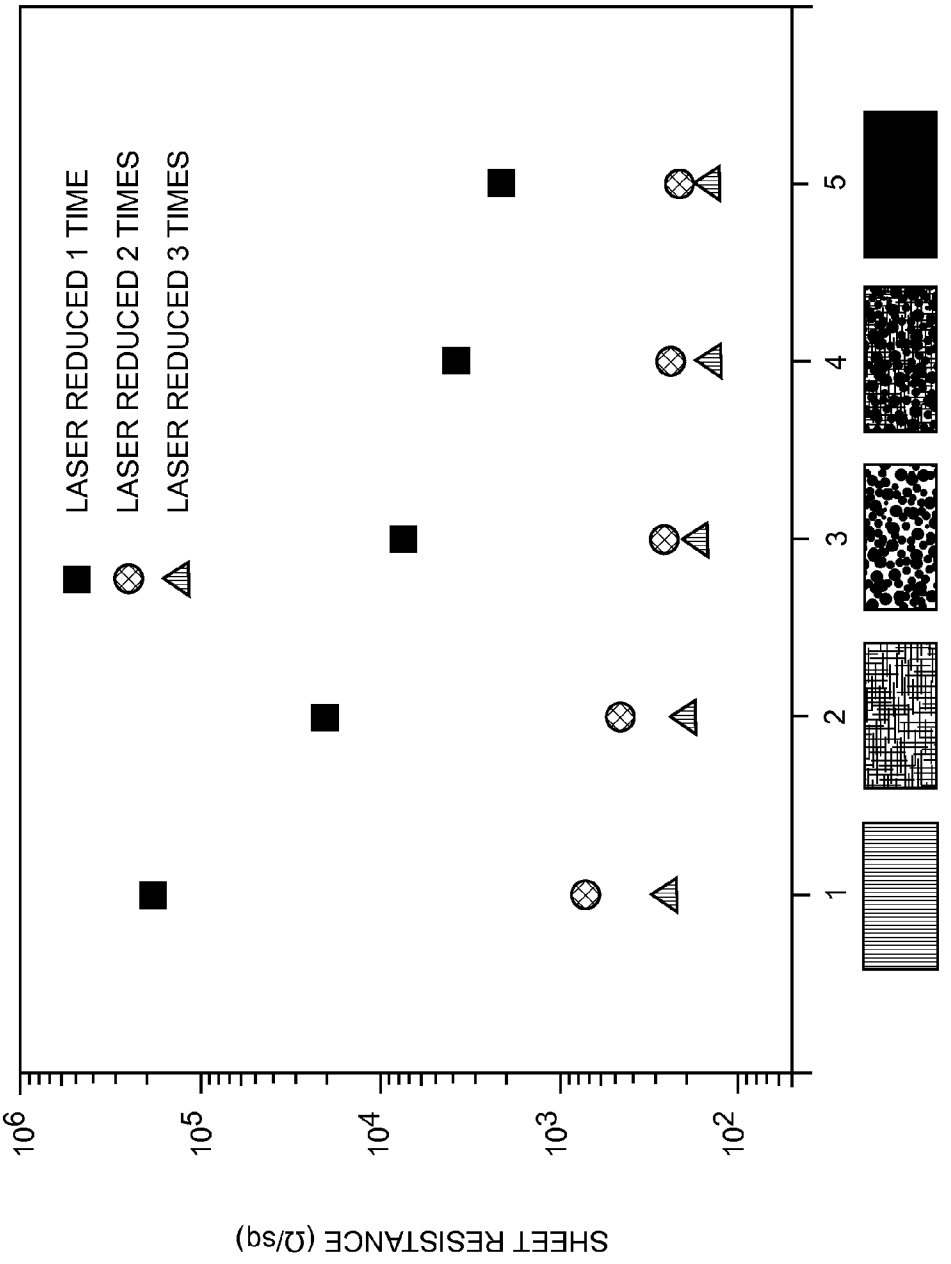
LASER REDUCED 1 TIME
LASER REDUCED 2 TIMES
LASER REDUCED 3 TIMES
SHEET RESISTANCE (Ω/sq)
10^6
10^5
10^4
10^3
10^2
1
2
3
4
5
GRAYSCALE LEVEL

FIG. 7

FIG. 8A

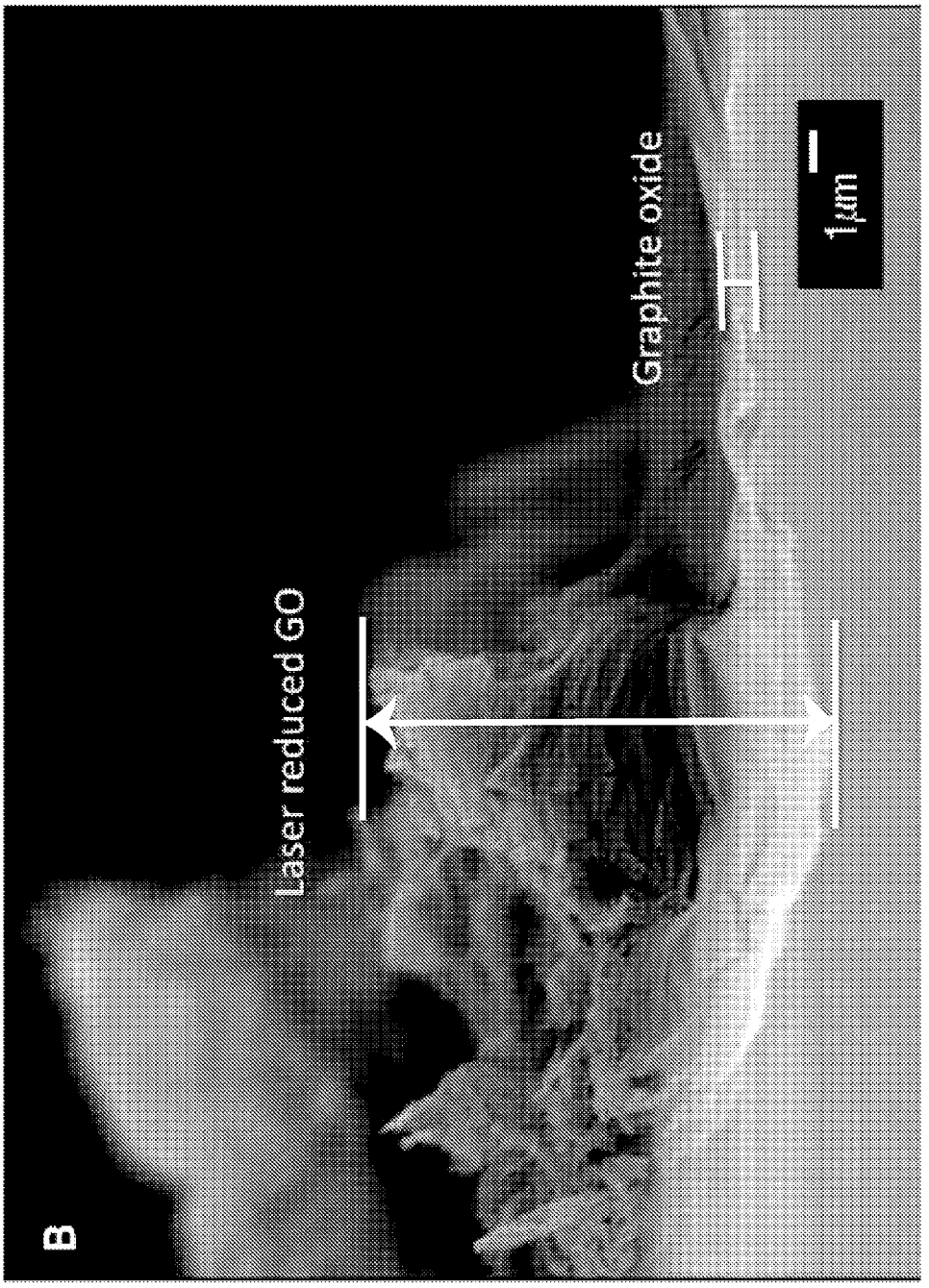

FIG. 8B

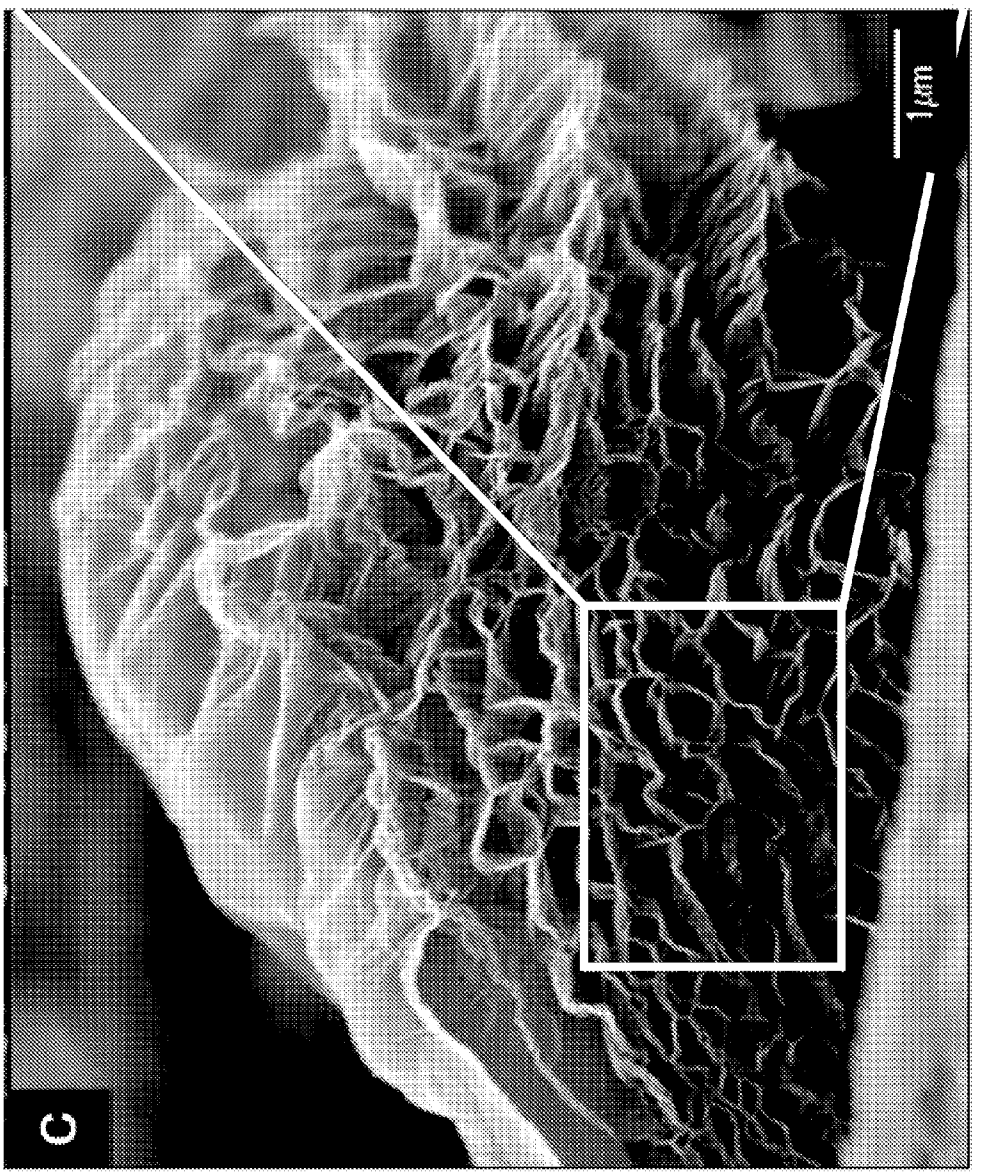

FIG. 8C

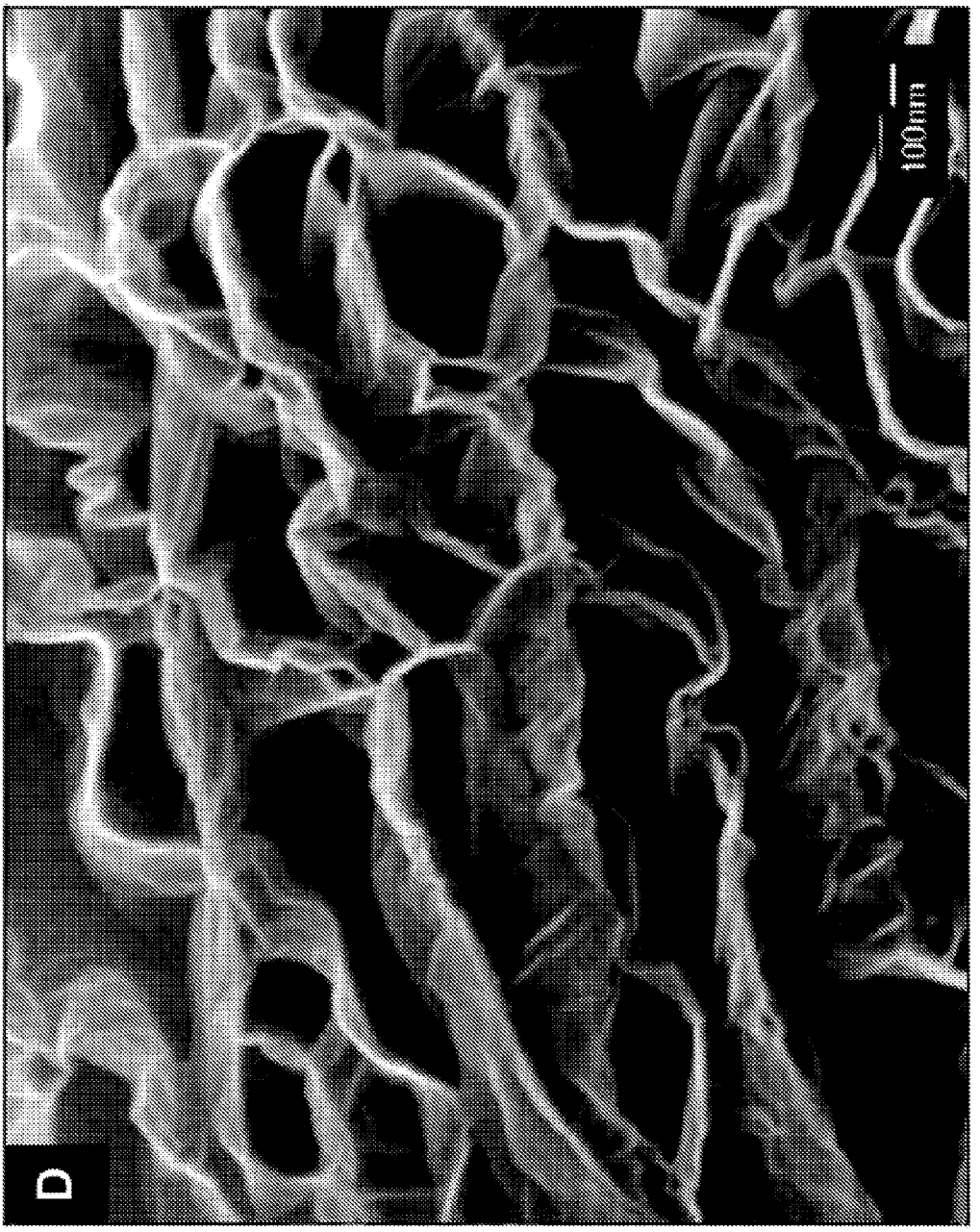

FIG. 8D

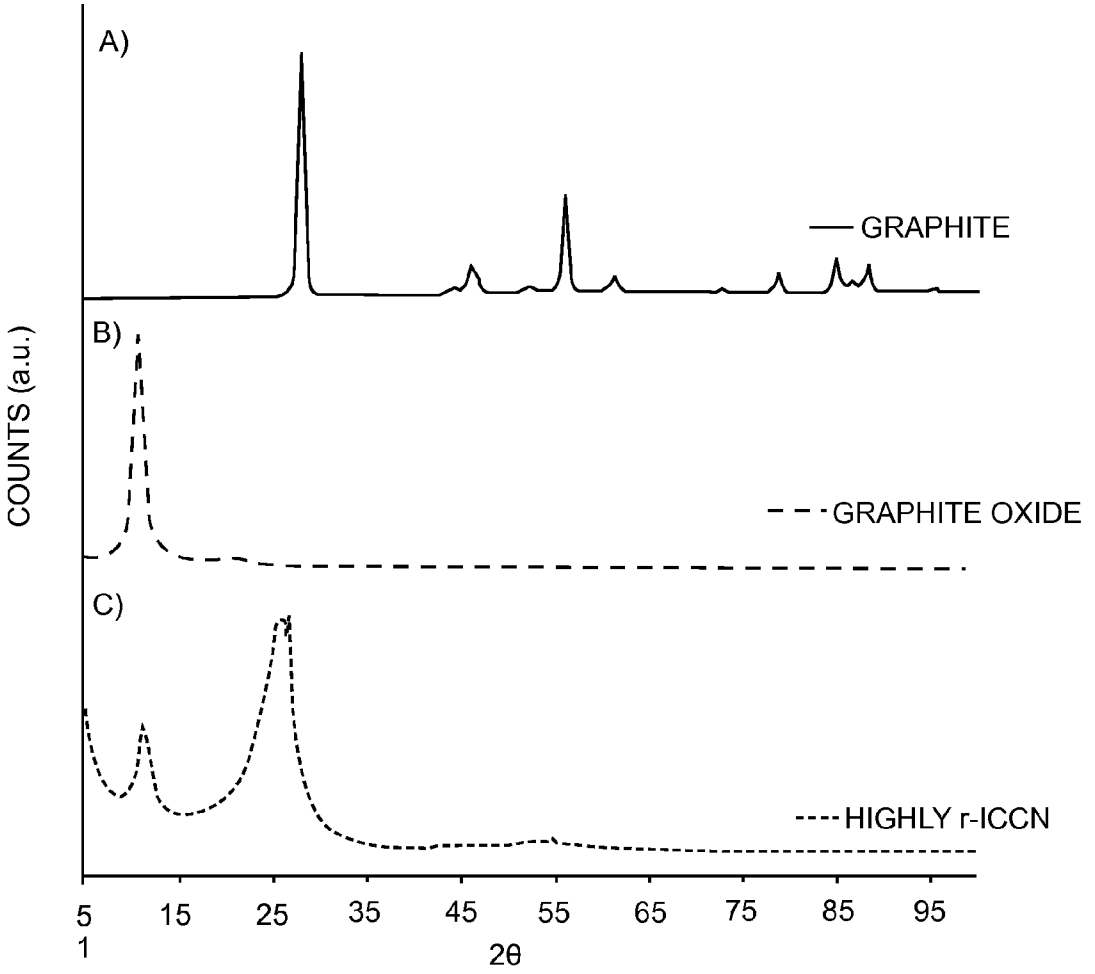
A)
GRAPHITE
B)
GRAPHITE OXIDE
C)
HIGHLY r-ICCN
COUNTS (a.u.)
5
15
25
35
45
55
65
75
85
95
1
2θ

FIG. 9

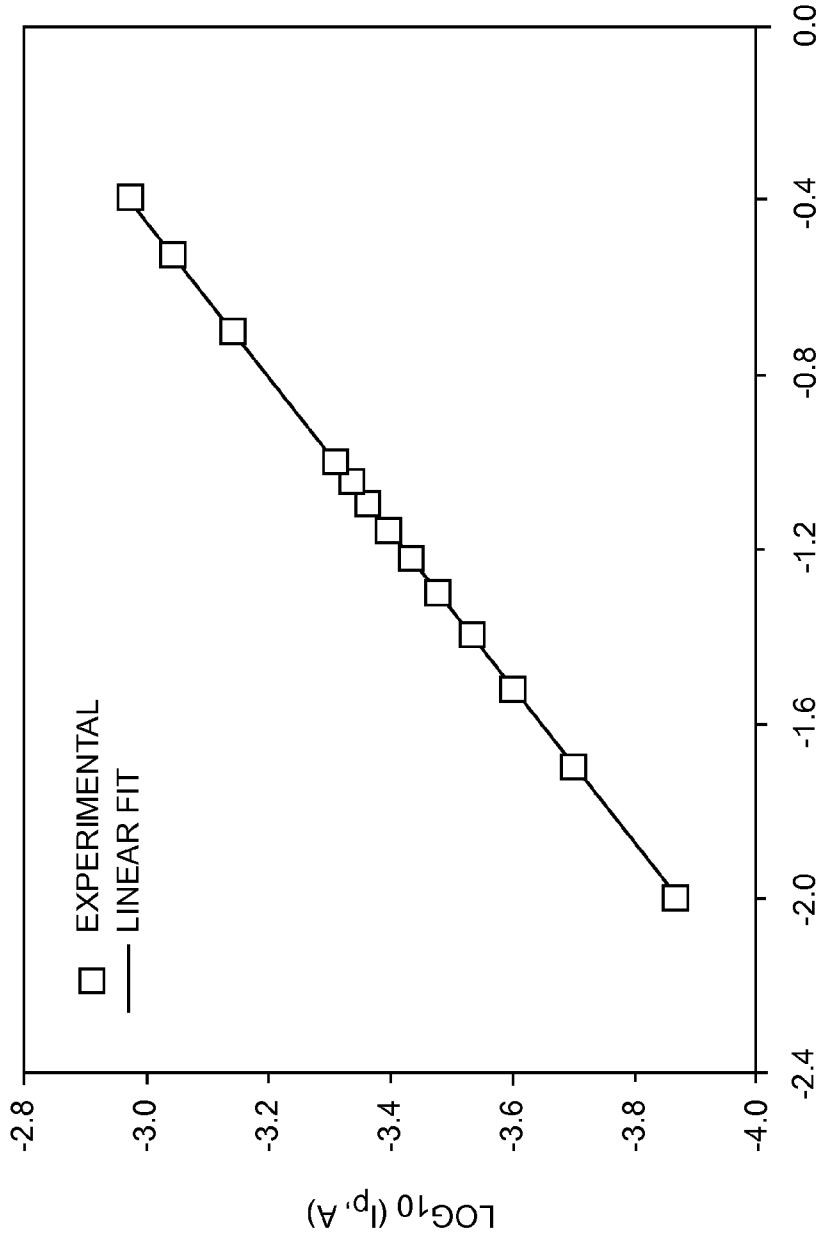
EXPERIMENTAL
LINEAR FIT
-2.8
-3.0
-3.2
-3.4
-3.6
-3.8
-4.0
LOG10 (Ip, A)
0.0
-0.4
-0.8
-1.2
-1.6
-2.0
-2.4
LOG10 (υ1 V/s)

FIG. 10

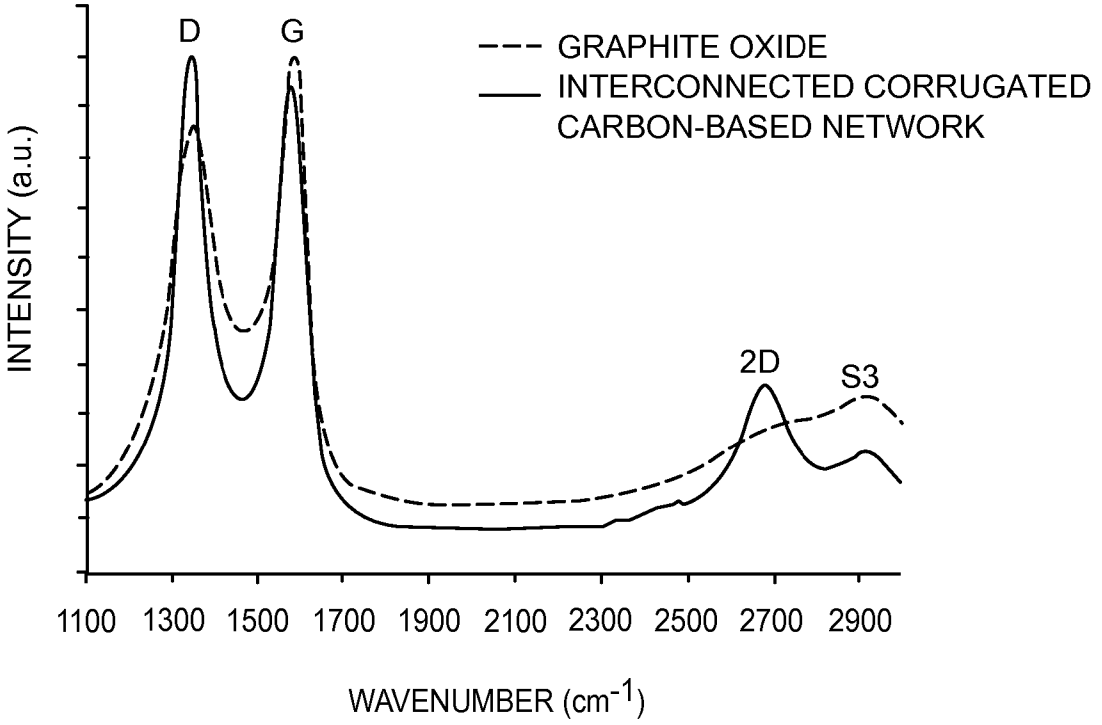
D
G
GRAPHITE OXIDE
INTERCONNECTED CORRUGATED CARBON-BASED NETWORK
2D
S3
INTENSITY (a.u.)
1100 1300 1500 1700 1900 2100 2300 2500 2700 2900
WAVENUMBER (cm-1)

FIG. 11A

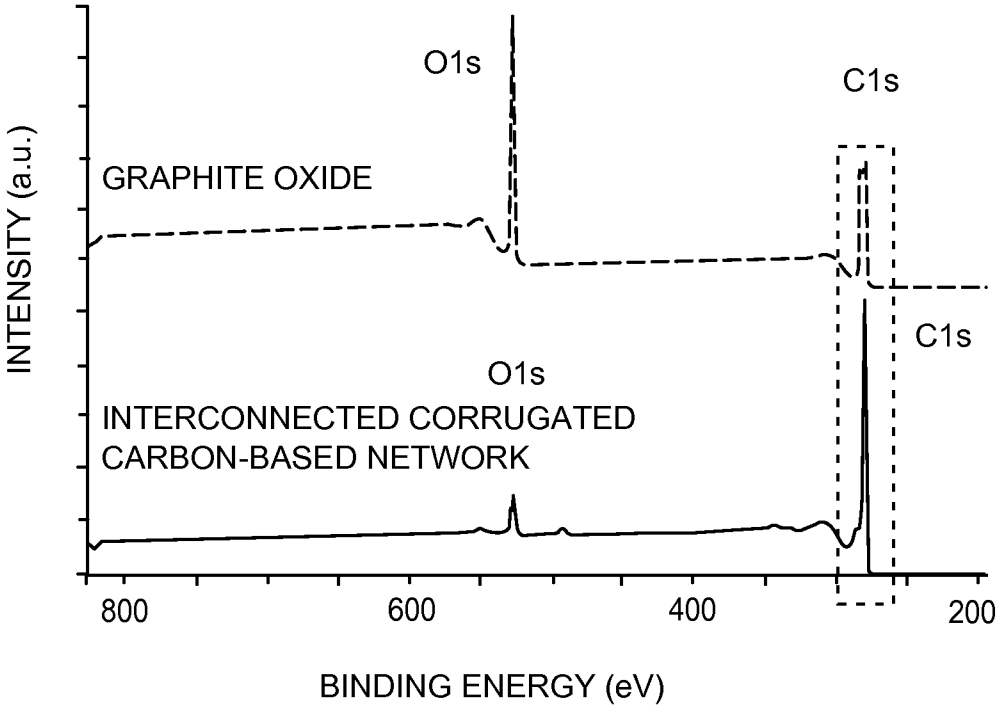
O1s
C1s
GRAPHITE OXIDE
C1s
O1s
INTERCONNECTED CORRUGATED
CARBON-BASED NETWORK
INTENSITY (a.u.)
800
600
400
200
BINDING ENERGY (eV)

FIG. 11B

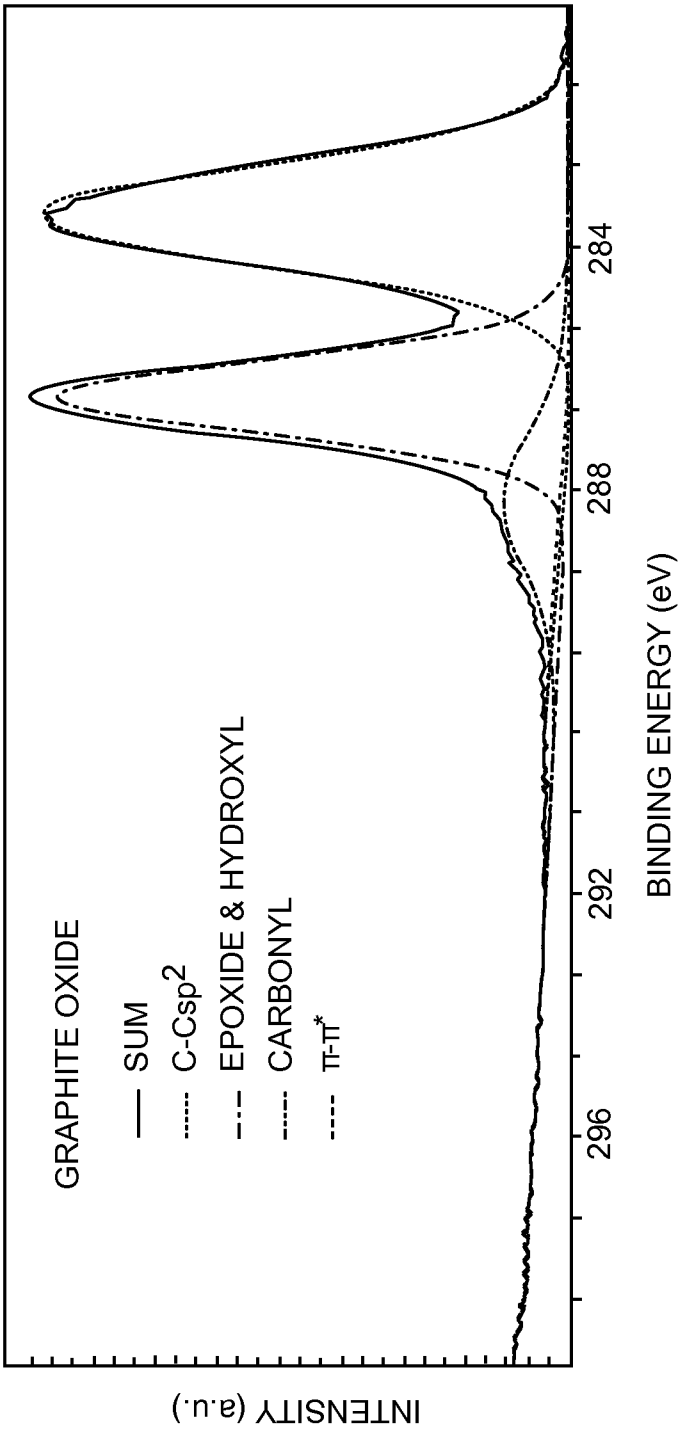
GRAPHITE OXIDE
SUM
C-Csp2
EPOXIDE & HYDROXYL
CARBONYL
π-π*
INTENSITY (a.u.)
284
288
292
296
BINDING ENERGY (eV)

FIG. 11C

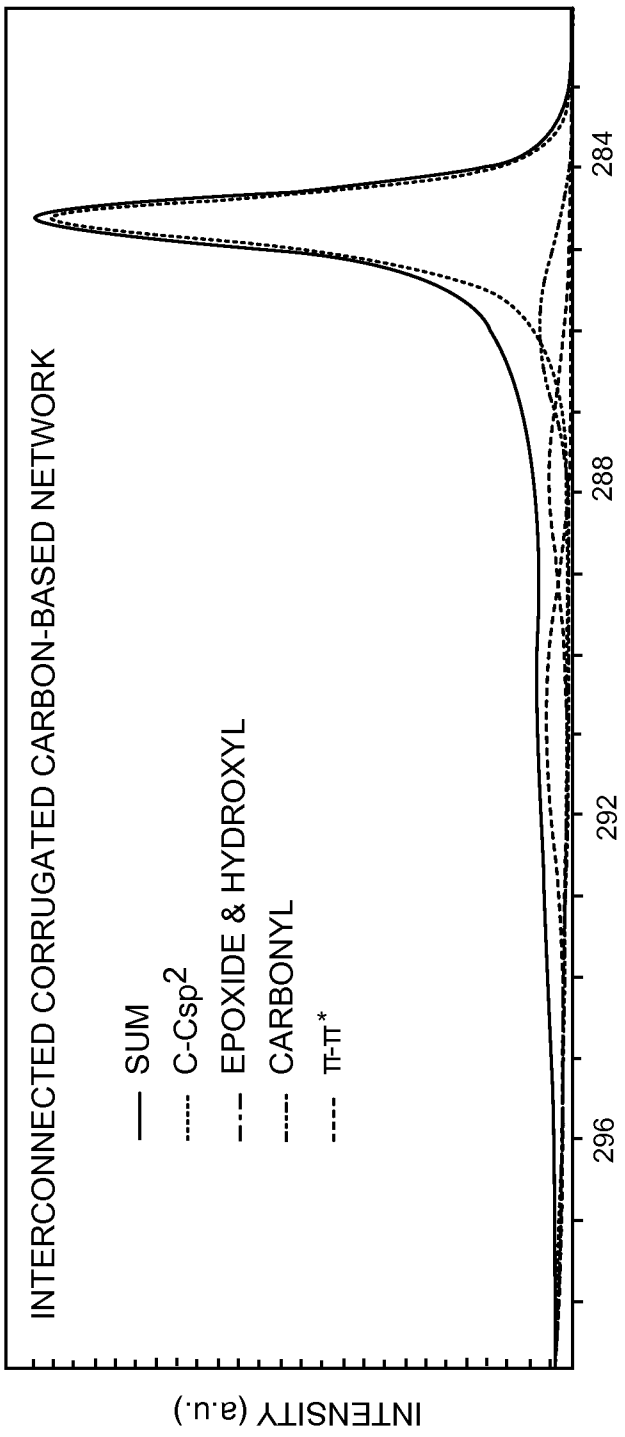
INTERCONNECTED CORRUGATED CARBON-BASED NETWORK
SUM
C-Csp2
EPOXIDE & HYDROXYL
CARBONYL
π-π*
INTENSITY (a.u.)
296
292
288
284
BINDING ENERGY (eV)

FIG. 11D

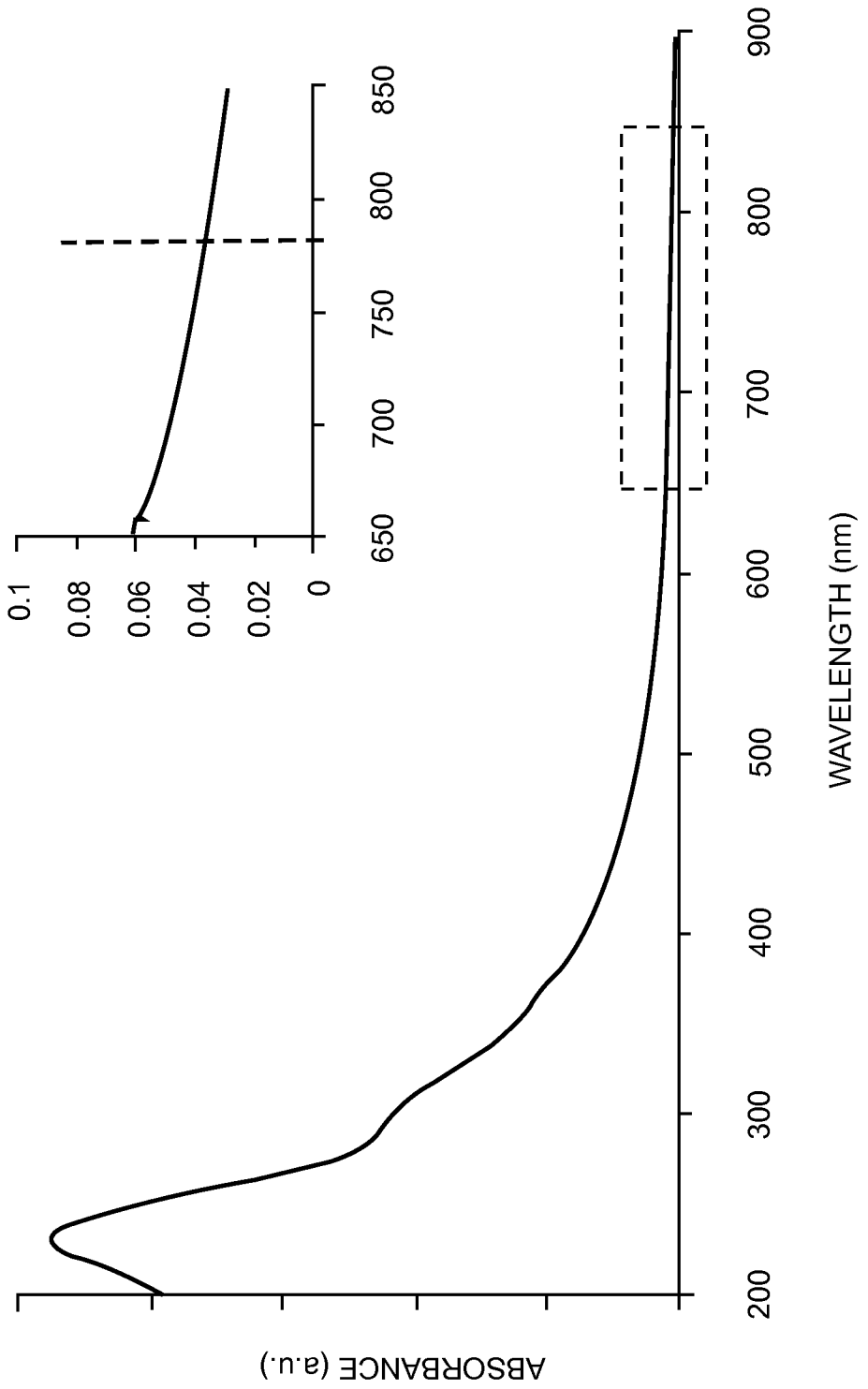
ABSORBANCE (a.u.)
WAVELENGTH (nm)
200
300
400
500
600
700
800
900
0
0.02
0.04
0.06
0.08
0.1
650
700
750
800
850

FIG. 11E

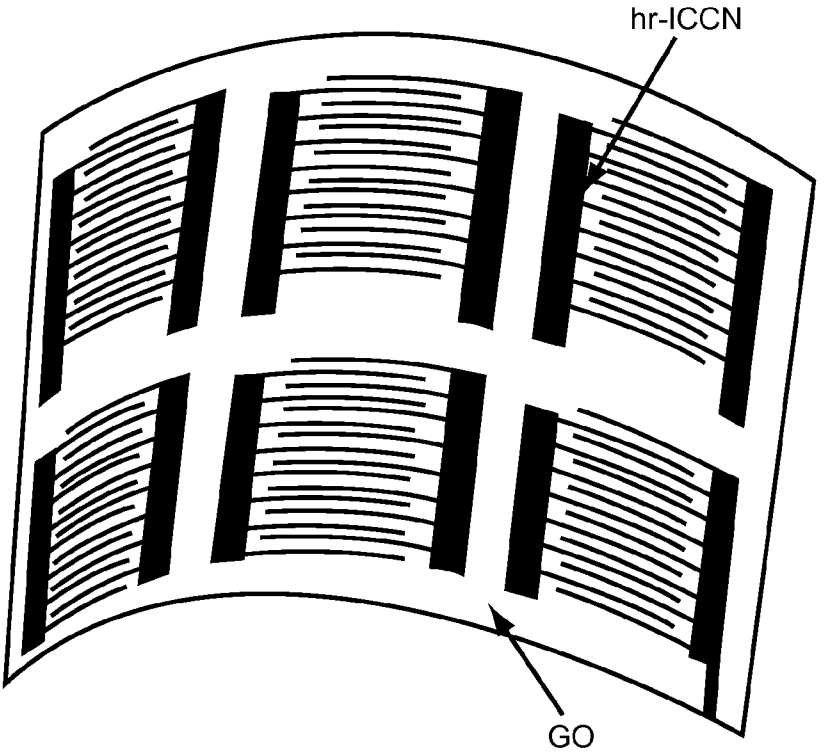

FIG. 12A

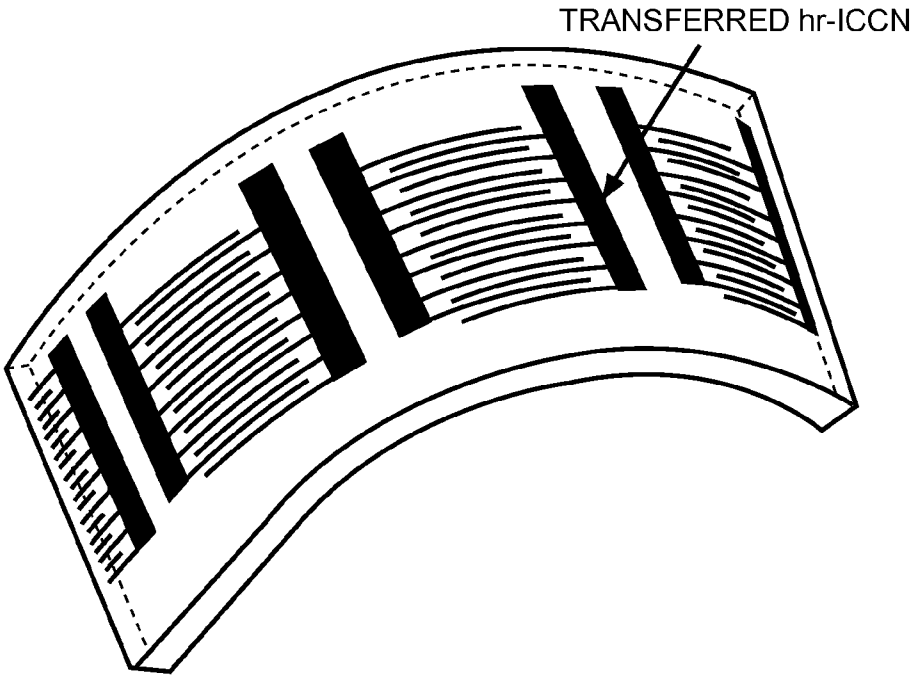

FIG. 12B

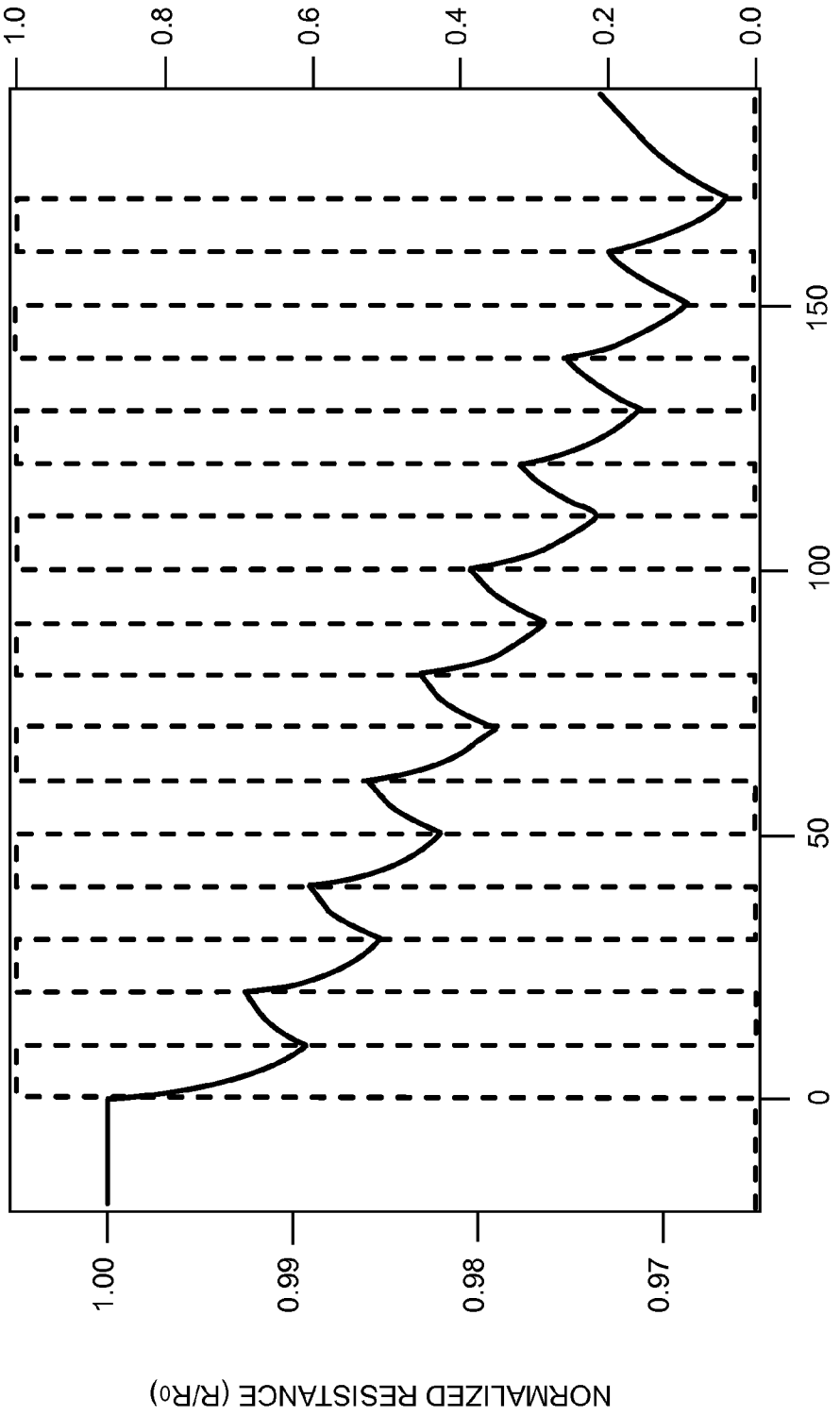
1.0
0.8
0.6
0.4
0.2
0.0
150
100
50
0
TIME (min)
1.00
0.99
0.98
0.97
NORMALIZED RESISTANCE (R/R0)

FIG. 13

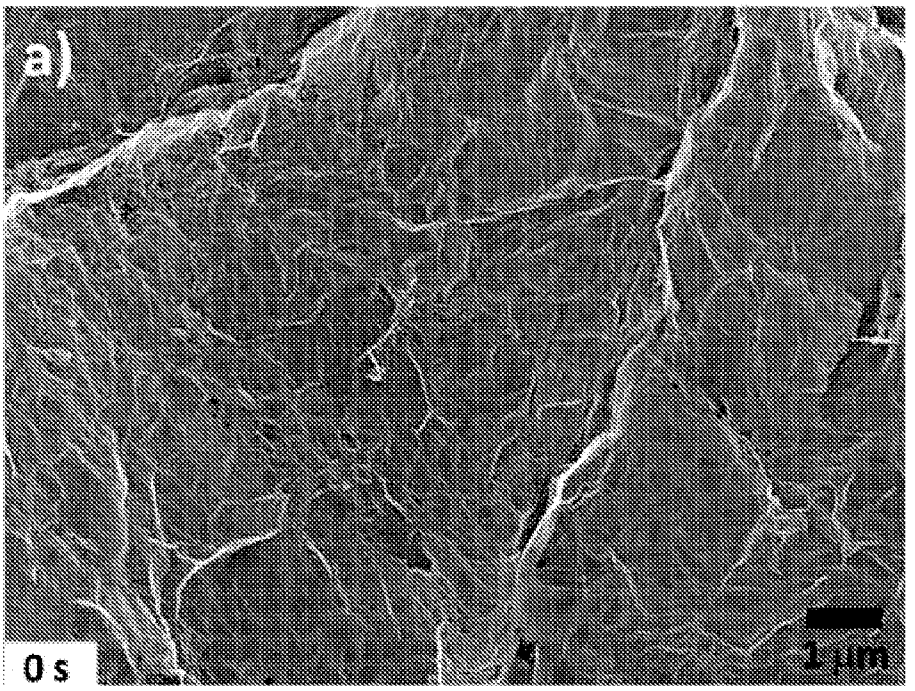

FIG. 14A

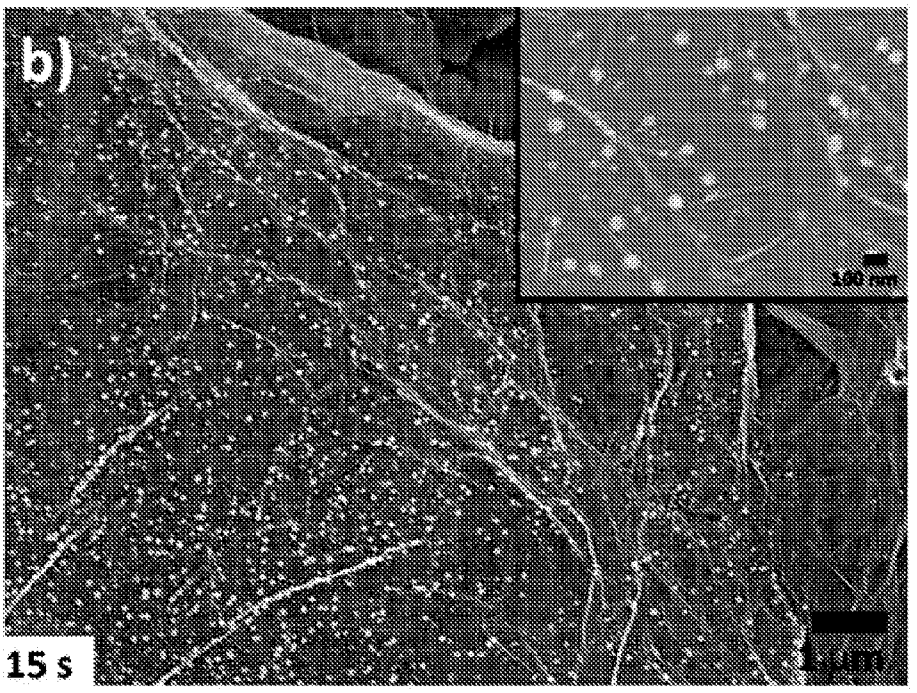

FIG. 14B

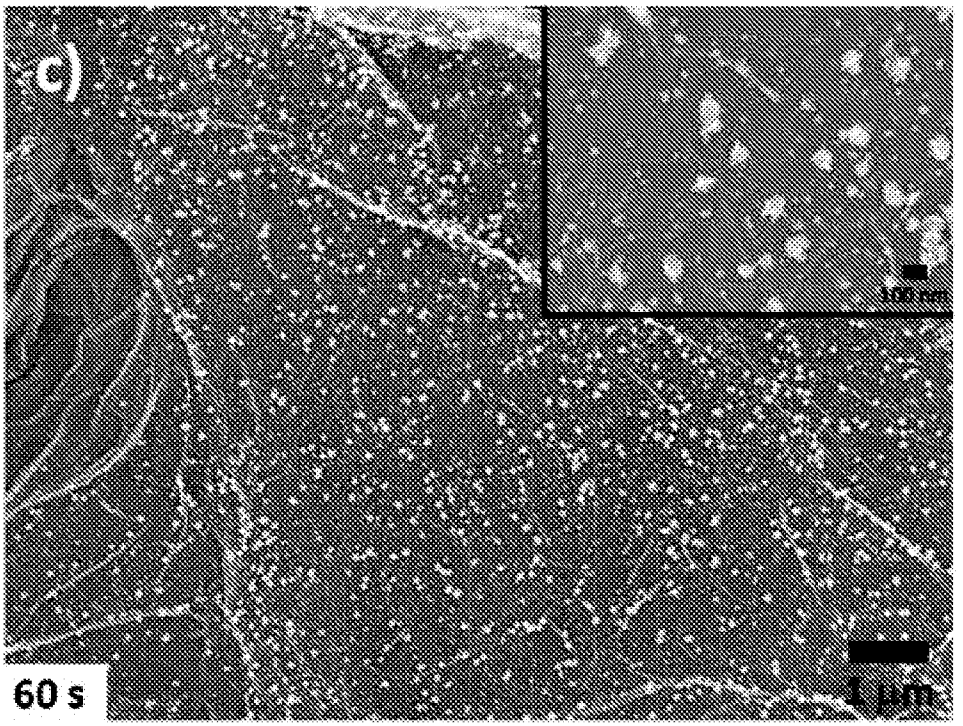

FIG. 14C

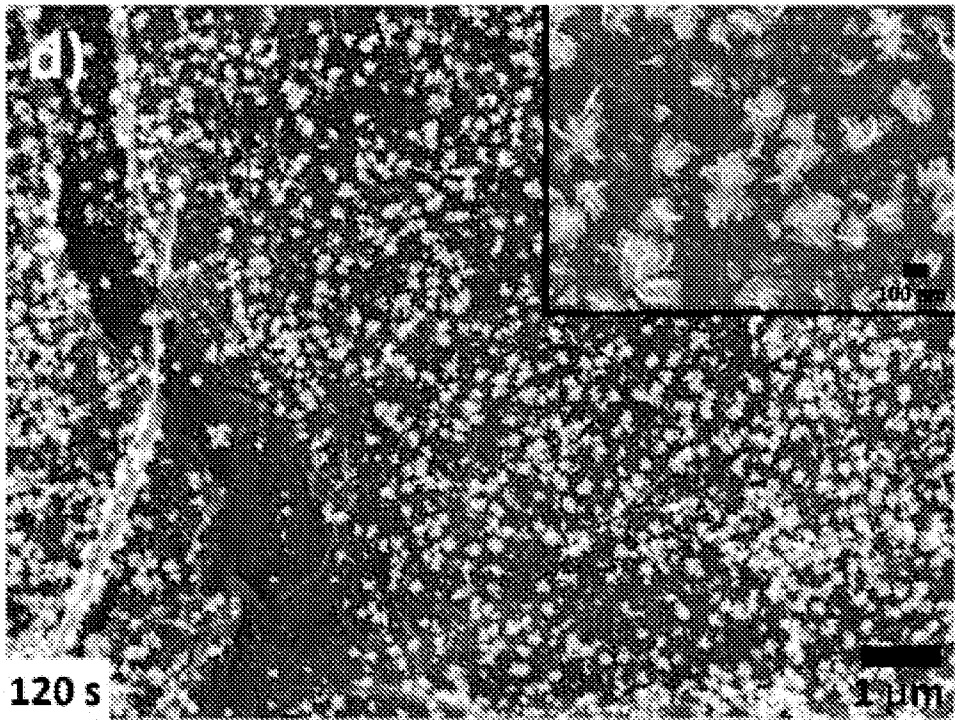

FIG. 14D

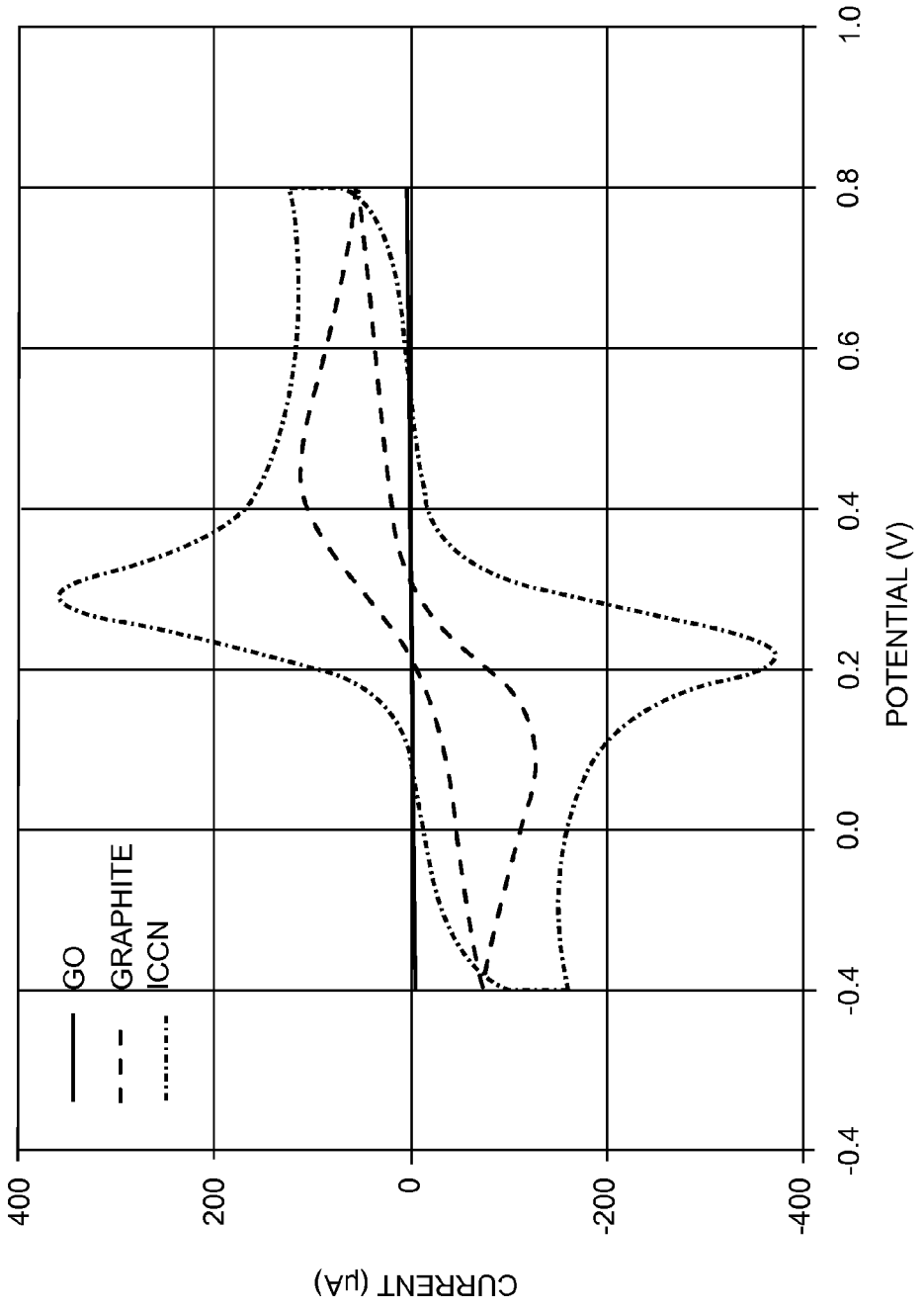
GO
GRAPHITE
ICCN
400
200
0
-200
-400
CURRENT (μA)
-0.4
0.0
0.2
0.4
0.6
0.8
1.0
POTENTIAL (V)

FIG. 15

INTERCONNECTED CORRUGATED CARBON-BASED NETWORK

RELATED APPLICATIONS

[0001] This application claims the benefit of U.S. provisional patent application No. 61/578,431, filed Dec. 21, 2011, the disclosure of which is incorporated herein by reference in its entirety.

[0002] This invention was made with Government support under Grant No. HR0011-10-3-0002, awarded by the United States Department of Defense, Defense Advanced Research Projects Agency. The Government has certain rights in this invention.

FIELD OF THE DISCLOSURE

[0003] The present disclosure provides an interconnected corrugated carbon-based network and an inexpensive process for making, patterning, and tuning the electrical, physical and electrochemical properties of the interconnected corrugated carbon-based network.

BACKGROUND

[0004] In the pursuit of producing high quality bulk carbon-based devices such as organic sensors, a variety of syntheses now incorporate graphite oxide (GO) as a precursor for the generation of large scale carbon-based materials. Inexpensive methods for producing large quantities of GO from the oxidation of graphitic powders are now available. In addition, the water dispersibility of GO combined with inexpensive production methods make GO an ideal starting material for producing carbon-based devices. In particular, GO has water dispersible properties. Unfortunately, the same oxygen species that give GO its water dispersible properties also create defects in its electronic structure, and as a result, GO is an electrically insulating material. Therefore, the development of device grade carbon-based films with superior electronic properties requires the removal of these oxygen species, re-establishment of a conjugated carbon network, as well as a method for controllably patterning carbon-based device features.

[0005] Methods for reducing graphite oxide have included chemical reduction via hydrazine, hydrazine derivatives, or other reducing agents, high temperature annealing under chemical reducing gases and/or inert atmospheres, solvothermal reduction, a combination of chemical and thermal reduction methods, flash reduction, and most recently, laser reduction of GO. Although several of these methods have demonstrated relatively high quality graphite oxide reduction, many have been limited by expensive equipment, high annealing temperatures and nitrogen impurities in the final product. As a result, of these difficulties, a combination of properties that includes high surface area and high electrical conductivity in an expanded interconnected carbon network has remained elusive. In addition, large scale film patterning via an all encompassing step for both GO reduction and patterning has proven difficult and has typically been dependent on photo-masks to provide the most basic of patterns. Therefore, what is needed is an inexpensive process for making and patterning an interconnected corrugated carbon-based network having a high surface area with highly tunable electrical conductivity and electrochemical properties.

SUMMARY

[0006] The present disclosure provides a method of producing an interconnected corrugated carbon-based network. The interconnected corrugated carbon-based network produced has a combination of properties that includes high surface area and high electrical conductivity in an expanded network of interconnected carbon layers.

[0007] In one embodiment, the method produces a patterned interconnected corrugated carbon-based network. In that particular embodiment, an initial step receives a substrate having a carbon-based oxide film. Once the substrate is received, a next step involves generating a light beam having a power density sufficient to reduce portions of the carbon-based oxide film to an interconnected corrugated carbon-based network. Another step involves directing the light beam across the carbon-based oxide film in a predetermined pattern via a computerized control system while adjusting the power density of the light beam via the computerized control system according to predetermined power density data associated with the predetermined pattern.

[0008] In one embodiment, the substrate is a disc-shaped, digital versatile disc (DVD) sized thin plastic sheet removably adhered to a DVD sized plate that includes a DVD centering hole. The DVD sized plate carrying the disc-shaped substrate is loadable into a direct-to-disc labeling enabled optical disc drive. A software program executed by the computerized control system reads data that defines the predetermined pattern. The computerized control system directs a laser beam generated by the optical disc drive onto the disc-shaped substrate, thereby reducing portions of the carbon-based oxide film to an electrically conductive interconnected corrugated carbon-based network that matches shapes, dimensions, and conductance levels dictated by the data of the predetermined pattern.

[0009] Those skilled in the art will appreciate the scope of the disclosure and realize additional aspects thereof after reading the following detailed description in association with the accompanying drawings.

BRIEF DESCRIPTION OF THE DRAWINGS

[0010] The accompanying drawings incorporated in and forming a part of this specification illustrate several aspects of the disclosure, and together with the description serve to explain the principles of the disclosure.

[0011] FIG. **1** depicts the label side of a prior art direct-to-disc labeling type CD/DVD disc.

[0012] FIG. **2** is a schematic of a prior art direct-to-disc labeling type optical disc drive.

[0013] FIG. **3** is a process diagram for an exemplary process for providing graphite oxide (GO) films on a substrate.

[0014] FIG. **4** is a process diagram for laser scribing an interconnected corrugated carbon-based network and then fabricating electrical components from the interconnected corrugated carbon-based network.

[0015] FIG. **5** is a line drawing of a sample of the interconnected corrugated carbon-based network of the present embodiments.

[0016] FIG. **6**A is an artwork image of a man's head covered with circuits.

[0017] FIG. **6**B is a photograph of a GO film after the artwork image of FIG. **6**A is directly patterned on the GO film using the laser scribing technique of the present disclosure.

[0018] FIG. **7** is a graph that provides a comparison between changes in electrical conductivity by reducing the GO film of FIG. **6**B by using various grayscale levels to laser scribe the artwork of FIG. **6**A to produce the patterned GO film of FIG. **6**B.

[0019] FIG. **8**A is a scanning electron microscope (SEM) image that illustrates an infrared laser's effect on GO film prior to laser treatment on the right side of the image in contrast to an aligned, interconnected corrugated carbon-based network on the left side of the image.

[0020] FIG. **8**B is an SEM image showing that an interconnected corrugated carbon-based network has a thickness that is approximately 10 times larger in comparison to that of untreated GO film.

[0021] FIG. **8**C is an SEM image showing a cross-sectional view of a single laser converted interconnected corrugated carbon-based network.

[0022] FIG. **8**D is an SEM image showing a greater magnification of a selected area within the interconnected corrugated carbon-based network in FIG. **8**C.

[0023] FIG. **9** compares a powder X-ray diffraction (XRD) pattern of the interconnected corrugated carbon-based network with both graphite and graphite oxide diffraction patterns.

[0024] FIG. **10** is a plot of $\log_{10}$ of peak current versus $\log_{10}$ of an applied voltammetric scan rate.

[0025] FIGS. **11**A-**11**E are graphs related to Raman spectroscopy analysis.

[0026] FIG. **12**A is a structural diagram showing a set of interdigitated electrodes made of interconnected corrugated carbon-based networks with dimensions of 6 mm×6 mm, spaced at ~500 μm, that are directly patterned onto a thin film of GO.

[0027] FIG. **12**B is a structural diagram showing the set of interdigitated electrodes transferred onto another type of substrate.

[0028] FIG. **13** shows the sensor response for a patterned flexible set of interdigitated electrodes that are made of interconnected corrugated carbon-based networks that are exposed to 20 ppm of nitrous oxide (NO_2) in dry air.

[0029] FIGS. **14**A-**14**D shows SEM images illustrating the growth of platinum (Pt) nanoparticles onto a scaffold made of an interconnected corrugated carbon-based network with respect to electrodeposition times corresponding to 0, 15, 60 and 120 seconds.

[0030] FIG. **15** compares the CV profiles of GO, graphite and electrodes made of interconnected corrugated carbon-based networks in an equimolar mixture of 5 mM $K_3[Fe(CN)_6]/K_4[Fe(CN)_6]$ dissolved in 1.0 M KCl solution at a scan rate of 50 mV/s.

DETAILED DESCRIPTION

[0031] The embodiments set forth below represent the necessary information to enable those skilled in the art to practice the disclosure and illustrate the best mode of practicing the disclosure. Upon reading the following description in light of the accompanying drawings, those skilled in the art will understand the concepts of the disclosure and will recognize applications of these concepts not particularly addressed herein. It should be understood that these concepts and applications fall within the scope of the disclosure and the accompanying claims.

[0032] The present disclosure provides an inexpensive process for making and patterning an interconnected corrugated carbon-based network having stringent requirements for a high surface area with highly tunable electrical conductivity and electrochemical properties. The embodiments described herein not only meet these stringent requirements, but provide direct control over the conductivity and patterning of interconnected corrugated carbon-based networks while creating flexible electronic devices in a single step process. Moreover, the production of these interconnected corrugated carbon-based networks does not require reducing agents, or expensive equipment. The simple direct fabrication of interconnected corrugated carbon-based networks on flexible substrates therefore simplifies the development of lightweight electronic devices. The interconnected corrugated carbon-based networks can be synthesized on various substrates, such as plastic, metal, and glass. Herein an all-organic NO_2 gas sensor, a fast redox active electrode, and a scaffold for the direct growth of platinum (Pt) nanoparticles are demonstrated.

[0033] In at least one embodiment, the interconnected corrugated carbon-based networks are conducting films produced using a common and inexpensive infrared laser that fits inside a compact disc/digital versatile disc (CD/DVD) optical drive unit that provides a direct-to-disc label writing function. LightScribe (Registered Trademark of Hewlett Packard Corporation) and Label Flash (Registered Trademark of Yamaha Corporation) are exemplary direct-to-disc labeling technologies that pattern text and graphics onto the surface of a CD/DVD disc. LightScribe DVD drives are commercially available for around $20 and the LightScribing process is controlled using a standard desktop computer.

[0034] FIG. **1** depicts the label side of a standard direct-to-disc labeling type CD/DVD disc **10** that includes a label area **12** and a clamping area **14** that surrounds a centering hole **16**. A dye film **18** covers the label area **12** and is sensitive to laser energy that is typically directed onto the label area **12** to produce a permanent visible image that may comprise graphics **20** and text **22**. A position tracking indicia **24** is usable by an optical disc drive (not shown) to accurately locate an absolute angular position of the CD/DVD disc **10** within the optical disc drive so that the graphics **20** and/or text **22** can be re-written to provide increased contrast. Moreover, the position tracking indicia **24** is usable by the optical disc drive to allow additional graphics and/or text to be written without undesirably overwriting the graphics **20** and/or text **22**.

[0035] FIG. **2** is a schematic of a prior art direct-to-disc labeling type optical disc drive system **26**. In this exemplary case, the CD/DVD disc **10** is depicted in cross-section and loaded onto a spindle assembly **28** that is driven by a CD/DVD spindle motor **30**. The label area **12** is shown facing a laser assembly **32** that includes a label writer laser (LWL) **34**, a lens **36**, and a focus actuator **38**. The LWL **34** is typically a laser diode. Exemplary specifications for the LWL **34** includes a maximum pulse optical power of 350 mW at 780 nm emission and a maximum pulse output power of 300 mW at 660 nm emission. A laser beam **40** emitted by the LWL **34** is focused by the lens **36** that is alternately translated towards and away from the LWL **34** by the focus actuator **38** in order to maintain focus of the laser beam **40** onto the label area **12** of the CD/DVD disc **10**. The laser beam **40** is typically focused to a diameter that ranges from around 0.7 μm to around 1 μm.

[0036] The laser assembly **32** is responsive to a control system **42** that provides control signals **44** through an optical drive interface (ODI) **46**. The control system **42** further

includes a central processor unit (CPU) **48** and a memory **50**. Label image data (LID) having information needed to realize a permanent image to be written onto the label area **12** of the CD/DVD disc **10** is processed by the CPU **48**, which in turn provides an LID stream signal **52** that pulses the LWL **34** on and off to heat the dye film **18** to realize the image defined by the LID.

[0037] The CPU **48** also processes the LID through the ODI **46** to provide a position control signal **54** to a radial actuator **56** that translates the laser assembly **32** in relation to the label area **12** in response to position information contained in the LID. In some versions of the present embodiments, the optical disc drive system **26** monitors the focus of the laser beam **40** with an optical receiver (not shown), so that the ODI **46** can generate a focus control signal **58** for the focus actuator **38**. The ODI **46** also provides a motor control signal **60** for the CD/DVD spindle motor **30** that maintains an appropriate rotation speed of the CD/DVD disc **10** while a label writing process is ongoing.

[0038] In some versions of the optical disc drive system **26** the LWL **34** is used exclusively for label writing directly to the label area **12** of the CD/DVD disc **10** and a separate laser diode (not shown) is used to write and/or read data to/from a data side **62** of the CD/DVD disc **10**. In other versions of the optical disc drive system **26**, the LWL **34** is used for label writing and data reading and/or writing. When the LWL **34** is used for data reading and/or writing, the CD/DVD disc **10** is flipped over to expose the data side **62** of the CD/DVD disc **10** to the laser beam **40**. In versions wherein the LWL **34** is also used as a data read/write laser, the laser assembly **32** includes optical pick-up components (not shown) such as a beam splitter and at least one optical receiver. The output power of the LWL **34** is typically around 3 mW during data read operations.

[0039] In order to use the optical disc drive system **26** to realize an inexpensive process for making and patterning an interconnected corrugated carbon-based network having a high surface area with highly tunable electrical conductivity and electrochemical properties, a carbon-based film is substituted for the dye film **18** (FIG. **1**). In one embodiment, graphite oxide (GO) is synthesized from high purity graphite powder using a modified Hummer's method. Dispersions of GO in water (3.7 mg/mL) are then used to make GO films on various substrates. Exemplary substrates include but are not limited to polyethylene terephthalate (PET), nitrocellulose membrane (with 0.4 μm pore size), aluminum foil, carbonized aluminum, copper foil, and regular copier paper.

[0040] Referring to FIG. **3**, a process **100** begins with providing graphite powder **64**. The graphite powder **64** undergoes an oxidation reaction using the modified Hummer's method to become GO **66** (step **102**). However, it is to be understood that other oxidation methods for producing GO are available and such methods are within the scope of the present disclosure. An exfoliation procedure produces exfoliated GO **68** (step **104**). The exfoliation procedure may be accomplished via ultrasonication. It is to be understood that the exfoliated GO **68** results from a partial exfoliation and not a complete exfoliation to a single layer of GO. The partial exfoliation is used to create a high accessible surface area that enables a fast redox response which enables a fast sensor response. Additionally, the partial exfoliation of GO **68** provides the high surface area for growing metal nanoparticles that could then be used in catalysis. A substrate **70** carries a GO film **72** that is produced by a deposition procedure that deposits the exfoliated GO **68** onto the substrate **70** (step **106**). In at least some embodiments, a GO film **72** is made by either drop-casting or vacuum filtering GO dispersions onto the substrate **70** that is the size of a CD/DVD disc. The GO film **72** is typically allowed to dry for 24 hours under ambient conditions. However, controlling conditions to expose the GO film **72** to a relatively lower humidity and relatively higher temperature will dry the GO film **72** relatively quickly. The term GO herein refers to graphite oxide.

[0041] Referring to FIG. **4**, individual ones of the GO film (s) **72** are then affixed to a substrate carrier **74**, which has dimensions similar to the CD/DVD disc **10** (FIG. **1**)(step **108**). The substrate carrier **74** carrying the substrate **70** with the GO film **72** is loaded into the optical disc drive system **26** (FIG. **2**) such that the GO film **72** faces the LWL **34** for laser treatment (step **110**). In this way, the present embodiments use the GO film **72** in place of the dye film **18** (FIG. **1**). It is to be understood that the substrate carrier **74** can be a rigid or semi-rigid disc onto which the GO film **72** can be fabricated directly. In that case, the substrate carrier **74** replaces the function of the substrate **70**.

[0042] Images **76** for realizing electrical components **78** are patterned in concentric circles, moving outward from the center of the substrate carrier **74** (step **112**). The laser irradiation process results in the removal of oxygen species and the reestablishment of sp^2 carbons. This causes a change in the conductivity of the GO film **72** with a typical resistance of >20 MO/sq to become a relatively highly conducting plurality of expanded and interconnected carbon layers that make up an interconnected corrugated carbon-based network **80**. The number of times the GO film **72** is laser treated results in a significant and controllable change in the conductivity of the interconnected corrugated carbon-based network **80**. The interconnected corrugated carbon-based network **80** has a combination of properties that include high surface area and high electrical conductivity in an expanded interconnected network of carbon layers. In one embodiment the plurality of expanded and interconnected carbon layers has a surface area of greater than 1400 m^2/g. In another embodiment, the plurality of expanded and interconnected carbon layers has a surface area of greater than 1500 m^2/g. In yet another embodiment, the surface area is around about 1520 m^2/g. In one embodiment, the plurality of expanded and interconnected carbon layers yields an electrical conductivity that is greater than about 1500 S/m. In another embodiment, the plurality of expanded and interconnected carbon layers yields an electrical conductivity that is greater than about 1600 S/m. In yet another embodiment, the plurality of expanded and interconnected carbon layers yields an electrical conductivity of around about 1650 S/m. In still another embodiment, the plurality of expanded and interconnected carbon layers yields an electrical conductivity that is greater than about 1700 S/m. In yet one more embodiment, the plurality of expanded and interconnected carbon layers yields an electrical conductivity of around about 1738 S/m. Moreover, in one embodiment, the plurality of expanded and interconnected carbon layers yields an electrical conductivity that is greater than about 1700 S/m and a surface area that is greater than about 1500 m^2/g. In another embodiment, the plurality of expanded and interconnected carbon layers yields an electrical conductivity of around about 1650 S/m and a surface area of around about 1520 m^2/g.

[0043] The electrical components **78** comprising electrodes **82** used in the fabrication of a device **84** are laser

irradiated 6 times before reaching the relatively high conductivity of around about 1738 S/m. The laser irradiation process takes about 20 minutes per cycle. Afterwards, the substrate **70** carrying the interconnected corrugated carbon-based network **80** and any remaining GO film **72** is removed from the substrate carrier **74** (step **114**). Next, the interconnected corrugated carbon-based network **80** is fabricated into the electrical components **78** that make up the device **84** (step **116**). In this exemplary case, portions of the interconnected corrugated carbon-based network **80** on the substrate **70** are cut into rectangular sections to make the electrical components **78**, which include the electrodes **82** formed from the interconnected corrugated carbon-based network **80**.

[0044] The interconnected corrugated carbon-based network **80** possesses a very low oxygen content of only 3.5%. In other embodiments, the oxygen content of the expanded and interconnected carbon layers ranges from around about 1% to around about 5%. FIG. **5** is a line drawing of a sample of the interconnected corrugated carbon-based network **80**, which is made up of the plurality of expanded and interconnected carbon layers that include corrugated carbon layers such as a single corrugated carbon sheet **86**. In one embodiment, each of the expanded and interconnected carbon layers comprises at least one corrugated carbon sheet that is one atom thick. In another embodiment, each of the expanded and interconnected carbon layers comprises a plurality of corrugated carbon sheets that are each one atom thick. The thickness of the interconnected corrugated carbon-based network **80**, as measured from cross-sectional scanning electron microscopy (SEM) and profilometry, was found to be around about 7.6 μm. In one embodiment, a range of thickness of the plurality of expanded and interconnected carbon layers making up the interconnected corrugated carbon-based network **80** is from around 7 μm to 8 μm.

[0045] As an illustration of the diversity in image patterning that is possible, a complex image formed by the direct laser reduction of GO is shown in FIGS. **6**A and **6**B. FIG. **6**A is an artwork image of a man's head covered with circuits. FIG. **6**B is a photograph of a GO film after the artwork image of FIG. **6**A is directly patterned on the GO film using the laser scribing technique of the present disclosure. Essentially, any part of the GO film that comes in direct contact with the 780 nm infrared laser is effectively reduced to an interconnected corrugated carbon-based network, with the amount of reduction being controlled by the laser intensity; a factor that is determined by power density of the laser beam impinging on the GO film. The resulting image of FIG. **6**B is an effective print of the original image of FIG. **6**A. However, in this case the image of FIG. **6**B is made up of various reductions of the GO film. As expected, the darkest black areas indicate exposure to the strongest laser intensities, while the lighter gray areas are only partially reduced. Since different grayscale levels directly correlate with the laser's intensity, it is possible to tune the electrical properties of the generated interconnected corrugated carbon-based network over five to seven orders of magnitude in sheet resistance (Ω/sq) by simply changing the grayscale level used during the patterning process. As illustrated in FIG. **7**, there is a clear relationship between sheet resistance, grayscale level and the number of times the GO film is laser irradiated. Control over conductivity from a completely insulating GO film, with a typical sheet resistance value of >20 MΩ/sq, to a conducting interconnected corrugated carbon-based network that registers a sheet resistance value of approximately 80 Ω/sq, which translates to a conductivity of ~1650 S/m, is possible. This method is sensitive enough to differentiate between similar grayscale levels as shown in the graph of FIG. **7**, where the sheet resistance varies significantly with only a small variation in grayscale level. In addition, the number of times a GO film is laser treated results in a significant and controllable change in sheet resistance. Each additional laser treatment lowers the sheet resistance as seen in FIG. **7**, where a film is laser irradiated once (black squares), twice (circles) and three times (triangles) with respect to the grayscale level. Therefore, the film's sheet resistance is tunable both by controlling the grayscale level used and the number of times the film is reduced by the laser, a property that has so far been difficult to control through other methods.

[0046] Scanning electron microscope (SEM) techniques are usable to understand the effects a low energy infrared laser has on the structural properties of GO film by comparing the morphological differences between an interconnected corrugated carbon-based network and untreated graphite oxide GO film. FIG. **8**A is an SEM image that illustrates the infrared laser's effect on GO film prior to laser treatment on the right side of the image in contrast to an aligned, interconnected corrugated carbon-based network on the left side of the image that occurs after being reduced with the infrared laser. The image not only gives a clear definition between the interconnected corrugated carbon-based network and untreated GO regions, but also demonstrates the level of precision possible when using this method as a means to pattern and reduce GO. The regions of interconnected corrugated carbon-based network, which result from the laser treatment, can be further analyzed through cross-sectional SEM.

[0047] FIG. **8**B is an SEM image showing a cross-sectional view of a free standing film of laser treated and untreated GO film, which shows a significant difference between GO film thicknesses. As indicated by the white brackets in FIG. **8**B, an interconnected corrugated carbon-based network increases in thickness by approximately 10 times in comparison to that of untreated GO film. Moreover, a range of thickness of the plurality of expanded and interconnected carbon layers is from around 7 μm to around 8 μm. In one embodiment, an average thickness of the plurality of expanded and interconnected carbon layers is around 7.6 μm. The increased thickness stems from rapid degassing of gases generated and released during laser treatment, similar to thermal shock, which effectively causes the reduced GO to expand and exfoliate as these gases rapidly pass through the GO film. FIG. **8**C is an SEM image showing a cross-sectional view of a single interconnected corrugated carbon-based network, which shows an expanded structure that is a characteristic of the interconnected corrugated carbon-based network of the present disclosure.

[0048] FIG. **8**D is an SEM image showing a greater magnification of a selected area within the corrugated carbon-based network in FIG. **8**C. The SEM image of FIG. **8**D allows the thickness of the plurality of expanded and interconnected carbon layers to be calculated to be between 5-10 nm. However, the number of carbon layers in the plurality of expanded and interconnected carbon layers making up the interconnected corrugated carbon-based network is above 100. In another embodiment the number of carbon layers in the plurality of expanded and interconnected carbon layers is greater than 1000. In yet another embodiment the number of carbon layers in the plurality of expanded and interconnected carbon layers is greater than 10,000. In still another embodiment, the

number of carbon layers in the plurality of expanded and interconnected carbon layers is greater than 100,000. The SEM analysis shows that although an infrared laser emission is only marginally absorbed by GO, enough power and focus (i.e., power density) can cause sufficient thermal energy to efficiently reduce, deoxygenate, expand, and exfoliate the GO film. Moreover, the surface area of the interconnected corrugated carbon-based network is greater than about 1500 m^2/g.

[0049] Since each of the carbon layers have a theoretical surface area of 2630 m^2/g, a surface greater than 1500 m^2/g indicates that almost all surfaces of the carbon layers are accessible. The interconnected corrugated carbon-based network has an electrical conductivity that is greater than 17 S/cm. The interconnected corrugated carbon-based network forms when some wavelength of light hits the surface of the GO, and is then absorbed to practically immediately convert to heat, which liberates carbon dioxide (CO_2). Exemplary light sources include but are not limited to a 780 nm laser, a green laser, and a flash lamp. The light beam emission of the light sources may range from near infrared to ultraviolet wavelengths. The typical carbon content of the interconnected corrugated carbon-based network is greater than 97% with less than 3% oxygen remaining. Some samples of the interconnected corrugated carbon-based network are greater than 99% carbon even though the laser reduction process is conducted in the air.

[0050] FIG. **9** compares a powder X-ray diffraction (XRD) pattern of the corrugated carbon-based network with both graphite and graphite oxide diffraction patterns. A typical XRD pattern for graphite, shown in FIG. **9** trace A, displays the characteristic peak of 2θ=27.8° with a d-spacing of 3.20 Å. An XRD pattern (FIG. **9**, trace B) for GO, on the other hand, exhibits a single peak of 2θ=10.76°, which corresponds to an interlayer d-spacing of 8.22 Å. The increased d-spacing in GO is due to the oxygen containing functional groups in graphite oxide sheets, which tend to trap water molecules between the basal planes, causing the sheets to expand and separate. The XRD pattern of the corrugated carbon-based network (FIG. **9**, trace C) shows the presence of both GO (10.76° 2θ) and a broad graphitic peak at 25.97° 2θ associated with a d-spacing of 3.43 Å, (FIG. **10**C). The GO presence in the corrugated carbon-based network is expected since the laser has a desirable penetration depth, which results in the reduction of only the top portion of the film with the bottom layer being unaffected by the laser. The small presence of GO is more prominent in thicker films, but begins to diminish in thinner films. In addition, one can also observe a partially obstructed peak at 26.66° 2θ, which shows a similar intensity to the broad 25.97° 2θ peak. Both of these peaks are considered graphitic peaks, which are associated to two different lattice spacing between basal planes.

[0051] It has been previously shown that the immobilization of carbon nanotubes (CNTs) on glassy carbon electrodes will result in a thin CNT film, which directly affects the voltammetric behavior of the CNT modified electrodes. In a ferro/ferrocyanide redox couple, the voltammetric current measured at the CNT modified electrode will likely have two types of contributions. The thin layer effect is a significant contributor to the voltammetric current. The thin layer effect stems from the oxidation of ferrocyanide ions, which are trapped between the nanotubes. The other contribution results from the semi-infinite diffusion of ferrocyanide towards the planar electrode surface. Unfortunately, the mechanistic information is not easily de-convoluted and requires knowledge of the film thickness.

[0052] In contrast, no thin layer effect is observed in association with the interconnected corrugated carbon-based network of the present disclosure. FIG. **10** is a plot of $\log_{10}$ of peak current versus $\log_{10}$ of an applied voltammetric scan rate. In this case, no thin layer effect is observed since the plot has a consistent slope of 0.53 and is linear. The slope of 0.53 is relatively close to theoretical values calculated using a semi-infinite diffusion model governed by the Randles-Sevcik equation:

$$i_p = 0.3443AC_o^*\sqrt{\frac{D_o\nu(nF)^3}{RT}}$$

[0053] Raman spectroscopy is used to characterize and compare the structural changes induced by laser treating GO film. FIGS. **11**A-**11**E are graphs related to Raman spectroscopic analysis. As can be seen in FIG. **11**A, characteristic D, G, 2D and S3 peaks are observed in both GO and the interconnected corrugated carbon-based network. The presence of the D band in both spectra suggests that carbon sp^3 centers still exist after reduction. Interestingly, the spectrum of the interconnected corrugated carbon-based network shows a slight increase in the D band peak at ~1350 cm^{-1}. This unexpected increase is due to a larger presence of structural edge defects and indicates an overall increase in the amount of smaller graphite domains. The result is consistent with SEM analysis, where the generation of exfoliated accordion-like graphitic regions (FIG. **5**) caused by the laser treatment creates a large number of edges. However the D band also shows a significant overall peak narrowing, suggesting a decrease in the types of defects in the interconnected corrugated carbon-based network. The G band experiences a narrowing and a decrease in peak intensity as well as a peak shift from 1585 to 1579 cm^{-1}. These results are consistent with the re-establishment of sp^2 carbons and a decrease in structural defects within the basal planes. The overall changes in the G band indicate a transition from an amorphous carbon state to a more crystalline carbon state. In addition, a prominent and shifted 2D peak from around about 2730 to around about 2688 cm^{-1} is seen after GO is treated with the infrared laser, indicating a considerable reduction of the GO film and strongly points to the presence of a few-layer interconnected graphite structure. In one embodiment, the 2D Raman peak for the interconnected corrugated carbon-based network shifts from around about 2700 cm^{-1} to around about 2600 cm^{-1} after the interconnected corrugated carbon-based network is reduced from a carbon-based oxide. Moreover, as a result of lattice disorder, the combination of D-G generates an S3 second order peak, which appears at 2927 cm^{-1} and, as expected, diminishes with decreasing disorder after infrared laser treatment. In some embodiments, the plurality of expanded and interconnected carbon layers has a range of Raman spectroscopy S3 second order peak that ranges from around about 2920 cm^{-1} to around about 2930 cm^{-1}. The Raman analysis demonstrates the effectiveness of treating GO with an infrared laser as a means to effectively and controllably produce the interconnected corrugated carbon-based network.

[0054] X-ray photoelectron spectroscopy (XPS) was employed to correlate the effects of laser irradiation on the

oxygen functionalities and to monitor the structural changes on the GO film. Comparing the carbon to oxygen (C/O) ratios between GO and the interconnected corrugated carbon-based network provides an effective measurement of the extent of reduction achieved using a simple low energy infrared laser. FIG. **11**B illustrates the significant disparity between the C/O ratios before and after laser treatment of the GO films. Prior to laser reduction, typical GO films have a C/O ratio of approximately 2.6:1, corresponding to a carbon/oxygen content of ~72% and 38%. On the other hand, the interconnected corrugated carbon-based network has an enhanced carbon content of 96.5% and a diminished oxygen content of 3.5%, giving an overall C/O ratio of 27.8:1. Since the laser reduction process takes place under ambient conditions, it is postulated that some of the oxygen present in the interconnected corrugated carbon-based network film is a result of the film having a static interaction with oxygen found in the environment.

[0055] FIG. **11**C shows that the C1s XPS spectrum of GO displays two broad peaks, which can be resolved into three different carbon components corresponding to the functional groups typically found on the GO surface, in addition to a small π to π^* peak at 290.4 eV. These functional groups include carboxyl, sp^3 carbons in the form of epoxide and hydroxyl, and sp^2 carbons, which are associated with the following binding energies: approximately 288.1, 286.8 and 284.6 eV, respectively.

[0056] FIG. **11**D shows expected results, in that the large degree of oxidation in GO results in various oxygen components in the GO C1s XPS spectrum. These results are in contrast to the interconnected corrugated carbon-based network, which shows a significant decrease in oxygen containing functional groups and an overall increase in the C—C sp^2 carbon peak. This points to an efficient deoxygenating process as well as the re-establishment of C═C bonds in the interconnected corrugated carbon-based network. These results are consistent with the Raman analysis. Thus, an infrared laser such as LWL **34** (FIG. **2**) is powerful enough to remove a majority of the oxygen functional groups, as is evident in the XPS spectrum of the interconnected corrugated carbon-based network, which only shows a small disorder peak and a peak at 287.6 eV. The latter corresponds to the presence of sp^3 type carbons suggesting that a small amount of carboxyl groups remain in the final product. In addition, the presence of a π to π^* satellite peak at ~290.7 eV indicates that delocalized π conjugation is significantly stronger in the interconnected corrugated carbon-based network as this peak is miniscule in the GO XPS spectrum. The appearance of the delocalized IF peak is a clear indication that conjugation in the GO film is restored during the laser reduction process and adds support that an sp^2 carbon network has been re-established. The decreased intensity of the oxygen containing functional groups, the dominating C═C bond peak and the presence of the delocalized π conjugation all indicate that a low energy infrared laser is an effective tool in the generation of the interconnected corrugated carbon-based network.

[0057] FIG. **11**E depicts UV-visible light absorbance spectra of GO shown in black. The inset shows a magnified view of the boxed area showing the absorbance of GO with respect to a 780 nm infrared laser in the 650 to 850 nm region.

[0058] The future development of multifunctional flexible electronics such as roll-up displays, photovoltaic cells, and even wearable devices presents new challenges for designing and fabricating lightweight, flexible energy storage devices.

[0059] Embodiments of the present disclosure also include other types of electrical and electronic devices. For example, FIG. **12**A shows a set of interdigitated electrodes with dimensions of 6 mm×6 mm, spaced at ~500 μm, that are directly patterned onto a thin film of GO. Prior to being patterned, the GO film was deposited on a thin flexible substrate, polyethylene terephthalate (PET), in order to fabricate a set of electrodes that are mechanically flexible. The top arrow points to the region of the interconnected corrugated carbon-based network that makes up the black interdigitated electrodes, while the bottom arrow points to the un-reduced golden colored GO film. Since the electrodes are directly patterned onto the GO film on a flexible substrate, the need for post-processing such as transferring the film to a new substrate is unnecessary. Although, if desired, a peel and stick method could be used to selectively lift-off the black interdigitated electrodes made of interconnected corrugated carbon-based networks with e.g. polydimethysiloxane (PDMS) and transfer it onto other types of substrates (FIG. **12**B). The simplicity of this method allows substantial control over pattern dimensions, substrate selectivity and electrical properties of the interconnected corrugated carbon-based network by controlling the laser intensity and thereby the amount of reduction in each film.

[0060] These interdigitated electrodes can, in turn, be used as an all-organic flexible gas sensor for the detection of NO_2. FIG. **13** shows the sensor response for a patterned flexible set of interdigitated electrodes made of interconnected corrugated carbon-based networks that are exposed to 20 ppm of NO_2 in dry air. This sensor was fabricated by patterning interconnected corrugated carbon-based networks to fabricate the active electrode and marginally reducing the area in between the electrodes to have a consistent sheet resistance of ~7775 ohms/sq. In this way, it is possible to bypass the use of metal electrodes and directly pattern both the electrode and the sensing material on the flexible substrate simultaneously. The plot relates NO_2 gas exposure to R/R_0, where R_0 is the sheet resistance at the initial state and NO_2 is the resistance of the interconnected corrugated carbon-based networks film after exposure to the gas. The film was exposed to NO_2 gas for 10 min followed immediately by purging with air for another 10 min. This process was then repeated nine more times for a total of 200 min. Even with a slightly lower sensitivity than more sophisticated and optimized sensors, the un-optimized sensor made up of interconnected corrugated carbon-based networks still shows good, reversible sensing for NO_2 and its easy fabrication makes it quite advantageous for these systems. The sensor made up of interconnected corrugated carbon-based networks for NO_2 holds promise for improving the fabrication of all-organic flexible sensor devices, at low cost by using inexpensive starting materials directly patterned with an inexpensive laser.

[0061] The high conductivity and increased surface area resulting from the plurality of expanded and interconnected carbon layers, makes interconnected corrugated carbon-based networks a viable candidate for use as a heterogeneous catalyst support for metal nanoparticles. In particular, the direct growth of Pt nanoparticles on interconnected corrugated carbon-based networks could aid in the improvement of methanol based fuel cells, which have shown enhanced device performance from large surface area and conducting carbon-based scaffolds. This disclosure demonstrates that an interconnected corrugated carbon-based network is a viable scaffold for the controllable growth of Pt nanoparticles. By electrochemically reducing 1 mM of K_2PtCl_4 with 0.5 M

H_2SO_4 at −0.25 V for different periods of time, it is possible to actively control the Pt particle size that is electrodeposited on the interconnected corrugated carbon-based network film. FIGS. **14**A-**14**D shows scanning electron microscopy images illustrating the growth of Pt nanoparticles with respect to electrodeposition times corresponding to 0, 15, 60 and 120 seconds. As expected, there are no Pt particles present at 0 seconds of electrodeposition (FIG. **14**A), but small Pt nanoparticles are clearly visible after just 15 seconds (FIG. **14**B) with nanoparticle sizes ranging from 10-50 nm (FIG. **14**B, inset). After 60 seconds of electrodeposition, larger Pt nanoparticles grow with particle sizes averaging 100 to 150 nm (FIG. **14**C). Finally, after 120 seconds, 200 to 300 nm particles are found evenly distributed across the surface of the interconnected corrugated carbon-based networks (FIG. **14**D). The active growth of Pt nanoparticles at controllable diameters on interconnected corrugated carbon-based networks could make a potentially useful hybrid material for applications that require metal nanoparticles, such as methanol fuel cells and gas phase catalysts. Moreover, if palladium (Pd) is deposited a sensor made of an interconnected corrugated carbon-based network could be used for sensors that detect hydrogen or for catalysis such as Suzuki coupling or Heck coupling.

[0062] Carbon electrodes have attracted tremendous interest for various electrochemical applications because of their wide potential window and good electrocatalytic activity for many redox reactions. Given its high surface area and flexibility and the fact that it is an all-carbon electrode, interconnected corrugated carbon-based networks could revolutionize electrochemical systems by making miniaturized and fully flexible devices. Here, understanding the electrochemical properties of interconnected corrugated carbon-based networks is highly beneficial to determining its potential for electrochemical applications. Recently, graphene's electrocatalytic properties have been demonstrated to stem, in large part, from the efficient electron transfer at its edges rather than its basal planes. In fact, it has been reported that graphene exhibits in certain systems electrocatalytic activity similar to that of edge plane highly ordered pyrolytic graphite. In addition to having a highly expanded network, an interconnected corrugated carbon-based network also displays a large amount of edge planes (Refer back to FIG. **5**), making it an ideal system for studying the role of edge planes on the electrochemistry of graphene-based nanomaterials.

[0063] In this regard, the electrochemical behavior associated with the electron transfer of flexible electrodes made of interconnected corrugated carbon-based networks using a $[Fe(CN)_6]^{3-/4-}$ couple as a redox probe is characterized. For example, FIG. **15** compares the CV profiles of GO, graphite and electrodes made of interconnected corrugated carbon-based networks in an equimolar mixture of 5 mM $K_3[Fe(CN)_6]/K_4[Fe(CN)_6]$ dissolved in 1.0 M KCl solution at a scan rate of 50 mV/s. Unlike GO and graphite, the electrode made of interconnected corrugated carbon-based networks approaches the behavior of a perfectly reversible system with a low ΔE_p (peak-to-peak potential separation) of 59.5 mV at a scan rate of 10 mV/s to 97.6 mV at a scan rate 400 mV/s. The low ΔE_p values approaches the calculated theoretical value of 59 mV. Given that ΔE_p is directly related to the electron transfer rate constant (k^0_{obs}), the low experimental value of ΔE_p indicates a very fast electron transfer rate. The calculated k^0_{obs} values vary from 1.266×10^{-4} cm s^{-1} for graphite and, as expected, increases for an interconnected corrugated carbon-based network to 1.333×10^{-2} cm s^{-1}.

[0064] The redox system that was used for the evaluation of the electron transfer kinetics was 5 mM $K_3[Fe(CN)_6]/K_4[Fe(CN)_6]$ (1:1 molar ratio) dissolved in 1.0 M KCl solution. To ensure a stable electrochemical response, the electrodes were first cycled for at least 5 scans before collecting the experimental data. The heterogeneous electron transfer rate constant (k^0_{obs}) was determined using a method developed by Nicholson, which relates the peak separation (ΔE_p) to a dimensionless kinetic parameter ψ, and consequently to k^0_{obs} according to the following equation:

$$k^0_{obs} = \psi\left[\sqrt{D_O \pi v\left(\frac{nF}{RT}\right)}\right]\left(\frac{D_R}{D_O}\right)^{\frac{\alpha}{2}}$$

where D_O and D_R are the diffusion coefficients of the oxidized and reduced species, respectively. The other variables include v—the applied scan rate, n—the number of electrons transferred in the reaction, F—the Faraday constant, R—the gas constant, T—the absolute temperature and α—the transfer coefficient. The diffusion coefficients of the oxidized and reduced species are typically similar; therefore, the term $(D_R/D_O)^{\alpha/2}$ is ~1. A diffusion coefficient (D_O) of 7.26×10^{-6} cm^2 s^{-1} was used for $[[Fe(CN)_6]^{3-/4-}$ in 1.0 M KCl.

[0065] In addition to the relatively large increase in the electron transfer rate at the electrode made of interconnected corrugated carbon-based networks (~two orders of magnitude times faster than a graphite electrode), there is also substantial electrochemical activity for the electrode made of interconnected corrugated carbon-based networks as seen by an increase of ~268% in the voltammetric peak current. These drastic improvements are attributed to the expanded architecture of interconnected corrugated carbon-based network films, which provide large open areas for the effective diffusion of the electroactive species and allow a better interfacial interaction with the interconnected corrugated carbon-based network surface. Additionally, it is surmised that the amount of edge-like surface per unit mass is thus, much higher than graphite, and therefore contributes to the higher electron transfer rates, as seen here. Given the large number of exposed edge sites in interconnected corrugated carbon-based networks, it is not surprising to find that it not only has a higher k^0_{obs} value than graphite, but surpasses that of carbon nanotube based electrodes and that of stacked graphene nanofibers.

[0066] Note that the electrodes made of interconnected corrugated carbon-based networks are fabricated on flexible PET substrates covered with GO which, when laser reduced, serves as both the electrode and the current collector, thus making this particular electrode not only lightweight and flexible, but also inexpensive. In addition, the low oxygen content in interconnected corrugated carbon-based networks (~3.5%) as shown through XPS analysis is quite advantageous to the electrochemical activity seen here, since a higher oxygen content at the edge plane sites have been shown to limit and slow down the electron transfer of the ferri-/ferrocyanide redox couple. As such, embodiments of the present disclosure provides methodologies for making highly electroactive electrodes for potential applications in vapor sensing, biosensing, electrocatalysis and energy storage.

[0067] The present disclosure relates to a facile, solid-state and environmentally safe method for generating, patterning, and electronic tuning of graphite-based materials at a low cost. Interconnected corrugated carbon-based networks are shown to be successfully produced and selectively patterned from the direct laser irradiation of GO films under ambient conditions. Circuits and complex designs are directly patterned on various flexible substrates without masks, templates, post-processing, transferring techniques, or metal catalysts. In addition, by varying the laser intensity and laser irradiation treatments the electrical properties of interconnected corrugated carbon-based networks are precisely tuned over five orders of magnitude, a feature that has proven difficult with other methods. This new mode of generating interconnected corrugated carbon-based networks provides a new venue for manufacturing all organic based devices such as gas sensors, and other electronics. The relatively inexpensive method for generating interconnected corrugated carbon-based networks on thin flexible organic substrates makes it a relatively ideal heterogeneous scaffold for the selective growth of metal nanoparticles. Moreover, the selective growth of metal nanoparticles has the potential in electrocatalysing methanol fuel cells. Further still, films made of interconnected corrugated carbon-based networks show exceptional electrochemical activity that surpasses other carbon-based electrodes in the electron charge transfer of ferro-/ferricyanide redox couple. The simultaneous reduction and patterning of GO through the use of an inexpensive laser is a new technique, which offers significant versatility for the fabrication of electronic devices, all organic devices, asymmetric films, microfluidic devices, integrated dielectric layers, batteries, gas sensor, and electronic circuitry.

[0068] In contrast to other lithography techniques, this process uses a low-cost infrared laser in an unmodified, commercially available CD/DVD optical disc drive with LightScribe technology to pattern complex images on GO and has the additional benefit to simultaneously produce the laser converted corrugated carbon network. A LightScribe technology laser is typically operated with a 780 nm wavelength at a power output within a range of around 5 mW to around 350 mW. However, it is to be under stood that as long as the carbon-based oxide absorbs within the spectrum of the laser's emission, the process is achievable at any wavelength at a given power output. This method is a simple, single step, low cost, and maskless solid-state approach to generating interconnected corrugated carbon-based networks that can be carried out without the necessity of any post-processing treatment on a variety of thin films. Unlike other reduction methods for generating graphite-based materials, this method is a non-chemical route and a relatively simple and environmentally safe process, which is not limited by chemical reducing agents.

[0069] The technique described herein is inexpensive, does not require bulky equipment, displays direct control over film conductivity and image patterning, can be used as a single step for fabricating flexible electronic devices, all without the necessity for sophisticated alignment or producing expensive masks. Also, due to the conductive nature of the materials used, it is possible to control the resulting conductivity by simply patterning at different laser intensities and power, a property that has yet to been shown by other methods. Working circuit boards, electrodes, capacitors, and/or conducting wires are precisely patterned via a computerized program. The technique allows control over a variety of parameters, and therefore provides a venue for simplifying device fabrication and has the potential to be scaled, unlike other techniques that are limited by cost or equipment. This method is applicable to any photothermically active material, which includes but is not limited to GO, conducting polymers, and other photothermically active compounds such as carbon nanotubes.

[0070] As described above, a method has been presented for producing graphite-based materials that is not only facile, inexpensive and versatile, but is a one step environmentally safe process for reducing and patterning graphite films in the solid state. A simple low energy, inexpensive infrared laser is used as a powerful tool for the effective reduction, subsequent expansion and exfoliation and fine patterning of GO. Aside from the ability to directly pattern and effectively produce large areas of highly reduced laser converted graphite films, this method is applicable to a variety of other thin substrates and has the potential to simplify the manufacturing process of devices made entirely from organic materials. A flexible all organic gas sensor has been fabricated directly by laser patterning of GO deposited on thin flexible PET. An interconnected corrugated carbon-based network is also shown to be an effective scaffold for the successful growth and size control of Pt nanoparticles via a simple electrochemical process. Finally, a flexible electrode made of interconnected corrugated carbon-based networks was fabricated, which displays a textbook-like reversibility with an impressive increase of ~238% in electrochemical activity when compared to graphite towards the electron transfer between the ferri-/ferrocyanide redox couple. This proof-of concept process has the potential to effectively improve applications that would benefit from the high electrochemical activity demonstrated here including batteries, sensors and electrocatalysis.

[0071] Those skilled in the art will recognize improvements and modifications to the embodiments of the present disclosure. All such improvements and modifications are considered within the scope of the concepts disclosed herein and the claims that follow.

What is claimed is:

1. An interconnected corrugated carbon-based network comprising a plurality of expanded and interconnected carbon layers.

2. The interconnected corrugated carbon-based network of claim **1** wherein each of the expanded and interconnected carbon layers comprises at least one corrugated carbon sheet that is one atom thick.

3. The interconnected corrugated carbon-based network of claim **1** wherein each of the expanded and interconnected carbon layers comprises a plurality of corrugated carbon sheet that are each one atom thick.

4. The interconnected corrugated carbon-based network of claim **1** wherein the plurality of expanded and interconnected carbon layers yields an electrical conductivity that is greater than about 1500 S/m.

5. The interconnected corrugated carbon-based network of claim **1** wherein the plurality of expanded and interconnected carbon layers yields an electrical conductivity that is greater than about 1600 S/m.

6. The interconnected corrugated carbon-based network of claim **1** wherein the plurality of expanded and interconnected carbon layers yields an electrical conductivity of around about 1650 S/m.

7. The interconnected corrugated carbon-based network of claim **1** wherein the plurality of expanded and interconnected carbon layers yields an electrical conductivity that is greater than about 1700 S/m.

8. The interconnected corrugated carbon-based network of claim **1** wherein the plurality of expanded and interconnected carbon layers yields an electrical conductivity of around about 1738 S/m.

9. The interconnected corrugated carbon-based network of claim **1** wherein the plurality of expanded and interconnected carbon layers has a surface area that is greater than around about 1000 square meters per gram (m^2/g).

10. The interconnected corrugated carbon-based network of claim **1** wherein the plurality of expanded and interconnected carbon layers has a surface area that is greater than around about 1500 m^2/g.

11. The interconnected corrugated carbon-based network of claim **1** wherein the plurality of expanded and interconnected carbon layers has a surface area of around about 1520 m^2/g.

12. The interconnected corrugated carbon-based network of claim **1** wherein the plurality of expanded and interconnected carbon layers yields an electrical conductivity that is greater than about 1700 S/m and a surface area that is about 1500 m^2/g.

13. The interconnected corrugated carbon-based network of claim **1** wherein the plurality of expanded and interconnected carbon layers yields an electrical conductivity of around about 1650 S/m and a surface area of around about 1520 m^2/g.

14. The interconnected corrugated carbon-based network of claim **1** wherein a second order disordered (2D) Raman peak for the interconnected corrugated carbon-based network shifts from around about 2730 cm^{-1} to around about 2688 cm^{-1} after the interconnected corrugated carbon-based network is reduced from a carbon-based oxide.

15. The interconnected corrugated carbon-based network of claim **1** wherein a 2D Raman peak for the interconnected corrugated carbon-based network shifts from around about 2700 cm^{-1} to around about 2600 cm^{-1} after the interconnected corrugated carbon-based network is reduced from a carbon-based oxide.

16. The interconnected corrugated carbon-based network of claim **1** wherein an average thickness of the plurality of expanded and interconnected carbon layers is around 7.6 μm.

17. The interconnected corrugated carbon-based network of claim **1** wherein a range of thickness of the plurality of expanded and interconnected carbon layers is from around about 7 μm to around about 8 μm.

18. The interconnected corrugated carbon-based network of claim **1** wherein an oxygen content of the expanded and interconnected carbon layers is around about 3.5%.

19. The interconnected corrugated carbon-based network of claim **1** wherein an oxygen content of the expanded and interconnected carbon layers ranges from around about 1% to around about 5%.

20. The interconnected corrugated carbon-based network of claim **1** wherein the plurality of expanded and interconnected carbon layers has a carbon to oxygen (C/O) ratio of approximately 27.8:1.

21. The interconnected corrugated carbon-based network of claim **1** wherein the plurality of expanded and interconnected carbon layers has a C/O ratio that ranges from around about 100:1 to 25:1.

22. The interconnected corrugated carbon-based network of claim **1** wherein the plurality of expanded and interconnected carbon layers has a sheet resistance that is tunable within a range of around about 20 megaohms per square to around about 80 ohms per square.

23. The interconnected corrugated carbon-based network of claim **1** wherein the plurality of expanded and interconnected carbon layers has a Raman spectroscopy S3 second order peak at about 2927 cm^{-1}.

24. The interconnected corrugated carbon-based network of claim **1** wherein the plurality of expanded and interconnected carbon layers has a range of Raman spectroscopy S3 second order peak that ranges from around about 2920 cm^{-1} to around about 2930 cm^{-1}.

25. The interconnected corrugated carbon-based network of claim **1** wherein a number of carbon layers in the plurality of expanded and interconnected carbon layers is greater than about 100.

26. The interconnected corrugated carbon-based network of claim **1** wherein a number of carbon layers in the plurality of expanded and interconnected carbon layers is greater than about 1000.

27. The interconnected corrugated carbon-based network of claim **1** wherein a number of carbon layers in the plurality of expanded and interconnected carbon layers is greater than about 10,000.

28. The interconnected corrugated carbon-based network of claim **1** wherein a number of carbon layers in the plurality of expanded and interconnected carbon layers is greater than about 100,000.

29. A method of producing a patterned interconnected corrugated carbon-based network comprising:

receiving a substrate having a carbon-based oxide film;

generating a light beam having a power density sufficient to reduce portions of the carbon-based oxide film to a plurality of expanded and interconnected carbon layers that are electrically conductive; and

directing the light beam across the carbon-based oxide film in a predetermined pattern via a computerized control system.

30. The method of claim **29** further including adjusting the power density of the light beam to tune electrical conductivity of the plurality of expanded and interconnected carbon layers produced when the carbon-based oxide film is exposed to the light beam.

31. The method of claim **29** wherein the plurality of expanded and interconnected carbon layers has a sheet resistance that is tunable within a range of around 20 megaohms per square to around 80 ohms per square.

32. The method of claim **29** wherein the carbon-based oxide film is a graphite oxide film.

33. The method of claim **32** wherein the graphite oxide film has a C/O ratio of approximately 2.6:1.

34. The method of claim **32** wherein portions of the graphite oxide film exposed to the light beam have a C/O ratio of approximately 27.8:1.

35. The method of claim **29** wherein the plurality of expanded and interconnected carbon layers have a C/O ratio that ranges from around 100:1 to 25:1.

36. The method of claim **29** wherein the light beam is a laser beam.

37. The method of claim **36** wherein the laser beam is an infrared laser beam having a wave-length of around 780 nm.

38. The method of claim **29** wherein light beam emission ranges from near infrared to ultraviolet wavelengths.

39. The method of claim **29** wherein the light beam has a power of around about 5 mW.

40. The method of claim **29** wherein the light beam has a power range from around about 5 mW to around about 350 mW.

41. The method of claim **29** further including loading the substrate into an automated laser patterning system before generating the light beam having the power density sufficient to reduce portions of the carbon-based oxide film to the interconnected corrugated carbon-based network.

42. The method of claim **29** wherein exposing the carbon-based oxide film to the light beam to form the predetermined pattern of interconnected corrugated carbon-based networks within the carbon-based oxide film is repeated over predetermined portions of the predetermined pattern to increase a graphite to carbon-based oxide ratio.

43. The method of claim **29** further including an initial step of drop-casting a carbon-based oxide solution onto the substrate.

44. The method of claim **29** wherein the substrate is polyethylene terephthalate (PET).

45. The method of claim **29** further including exposing the substrate with oxygen plasma for around about three minutes.

46. The method of claim **29** wherein the plurality of expanded and interconnected carbon layers has a surface area of around about 1520 square meters per gram (m^2/g).

47. The method of claim **29** wherein each of the expanded and interconnected carbon layers is a single corrugated carbon sheet that is only one atom thick.

48. The method of claim **29** wherein the plurality of expanded and interconnected carbon layers yields an electrical conductivity that is greater than around about 1500 S/m.

49. The method of claim **29** wherein the plurality of expanded and interconnected carbon layers yields an electrical conductivity that is greater than around about 1600 S/m.

50. The method of claim **29** wherein the plurality of expanded and interconnected carbon layers yields an electrical conductivity of around about 1650 S/m.

51. The method of claim **29** wherein the plurality of expanded and interconnected carbon layers yields an electrical conductivity that is greater than about 1700 S/m.

52. The method of claim **29** wherein the plurality of expanded and interconnected carbon layers yields an electrical conductivity of around about 1738 S/m.

53. The method of claim **29** wherein the plurality of expanded and interconnected carbon layers has a surface area that is greater than around about 1000 m^2/g.

54. The method of claim **29** wherein the plurality of expanded and interconnected carbon layers has a surface area that is greater than around about 1500 m^2/g.

55. The method of claim **29** wherein the plurality of expanded and interconnected carbon layers has a surface area of around about 1520 m^2/g.

56. The method of claim **29** wherein the plurality of expanded and interconnected carbon layers yields an electrical conductivity that is greater than around about 1700 S/m and a surface area that is around about 1500 m^2/g.

57. The method of claim **29** wherein the plurality of expanded and interconnected carbon layers yields an electrical conductivity of around about 1650 S/m and a surface area of around about 1520 m^2/g.

58. The method of claim **29** wherein a second order disordered (2D) Raman peak for the interconnected corrugated carbon-based network shifts from around about 2730 cm^{-1} to around about 2688 cm^{-1} after the interconnected corrugated carbon-based network is reduced from a carbon-based oxide.

59. The method of claim **29** wherein a 2D Raman peak for the interconnected corrugated carbon-based network shifts from around about 2700 cm^{-1} to around about 2600 cm^{-1} after the interconnected corrugated carbon-based network is reduced from a carbon-based oxide.

60. The method of claim **29** wherein an average thickness of the plurality of expanded and interconnected carbon layers is around about 7.6 μm.

61. The method of claim **29** wherein a range of thickness of the plurality of expanded and interconnected carbon layers is from around about 7 μM to around about 8 μm.

62. The method of claim **29** wherein an oxygen content of the expanded and interconnected carbon layers is around about 3.5%.

63. The method of claim **29** wherein an oxygen content of the expanded and interconnected carbon layers ranges from around about 1% to around about 5%.

64. The method of claim **29** wherein the plurality of expanded and interconnected carbon layers have a C/O ratio of approximately 27.8:1.

65. The method of claim **29** wherein the plurality of expanded and interconnected carbon layers have a C/O ratio that ranges from around about 100:1 to 25:1.

66. The method of claim **29** wherein the plurality of expanded and interconnected carbon layers has a sheet resistance that is tunable within a range of around about 20 megaohms per square to around about 80 ohms per square.

67. The method of claim **29** wherein the plurality of expanded and interconnected carbon layers has a Raman spectroscopy S3 second order peak at around about 2927 cm^{-1}.

68. The method of claim **29** wherein the plurality of expanded and interconnected carbon layers has a range of Raman spectroscopy S3 second order peak that ranges from around about 2920 cm^{-1} to around about 2930 cm^{-1}.

69. The method of claim **29** wherein a number of carbon layers in the plurality of expanded and interconnected carbon layers is greater than around about 100.

70. The method of claim **29** wherein a number of carbon layers in the plurality of expanded and interconnected carbon layers is greater than around about 1000.

71. The method of claim **29** wherein a number of carbon layers in the plurality of expanded and interconnected carbon layers is greater than around about 10,000.

72. The method of claim **29** wherein a number of carbon layers in the plurality of expanded and interconnected carbon layers is greater than around about 100,000.

73. The method of claim **29** wherein the predetermined pattern defines conductive traces of an all-organic gas sensor.

74. The method of claim **73** wherein the all-organic gas sensor is a physically flexible nitrous oxide (NO_2) sensor.

75. The method of claim **29** wherein the predetermined pattern defines a fast redox active electrode.

76. The method of claim **29** wherein the predetermined pattern defines a scaffold for direct growth of nanoparticles.

77. The method of claim **76** wherein the nanoparticles are platinum (Pt) nanoparticles.

* * * * *